

**University of
Pennsylvania**

April 16, 2007



GALAXY **Simulations, Observations,**
MERGERS: **and Active Galactic Nuclei**

**Joel R. Primack (UCSC)
Thomas J. Cox (UCSC→CfA)
Patrik Jonsson (UCSC)
Jennifer Lotz (UCSC→Arizona)**

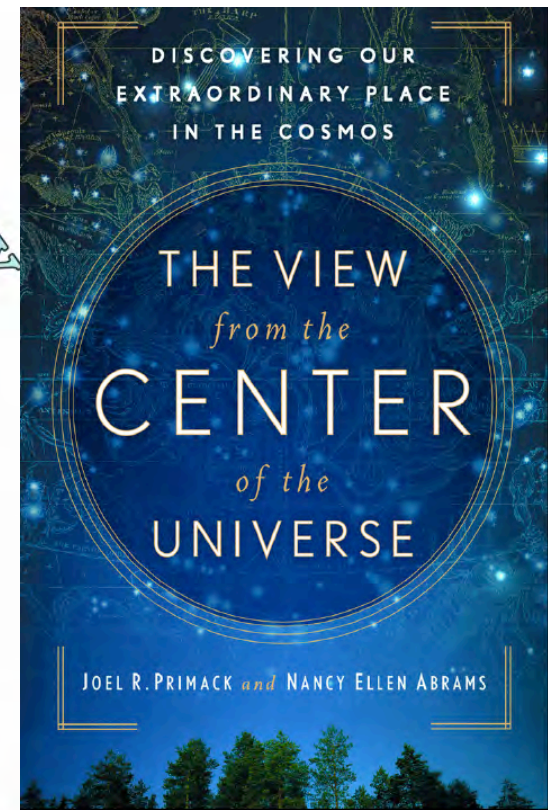
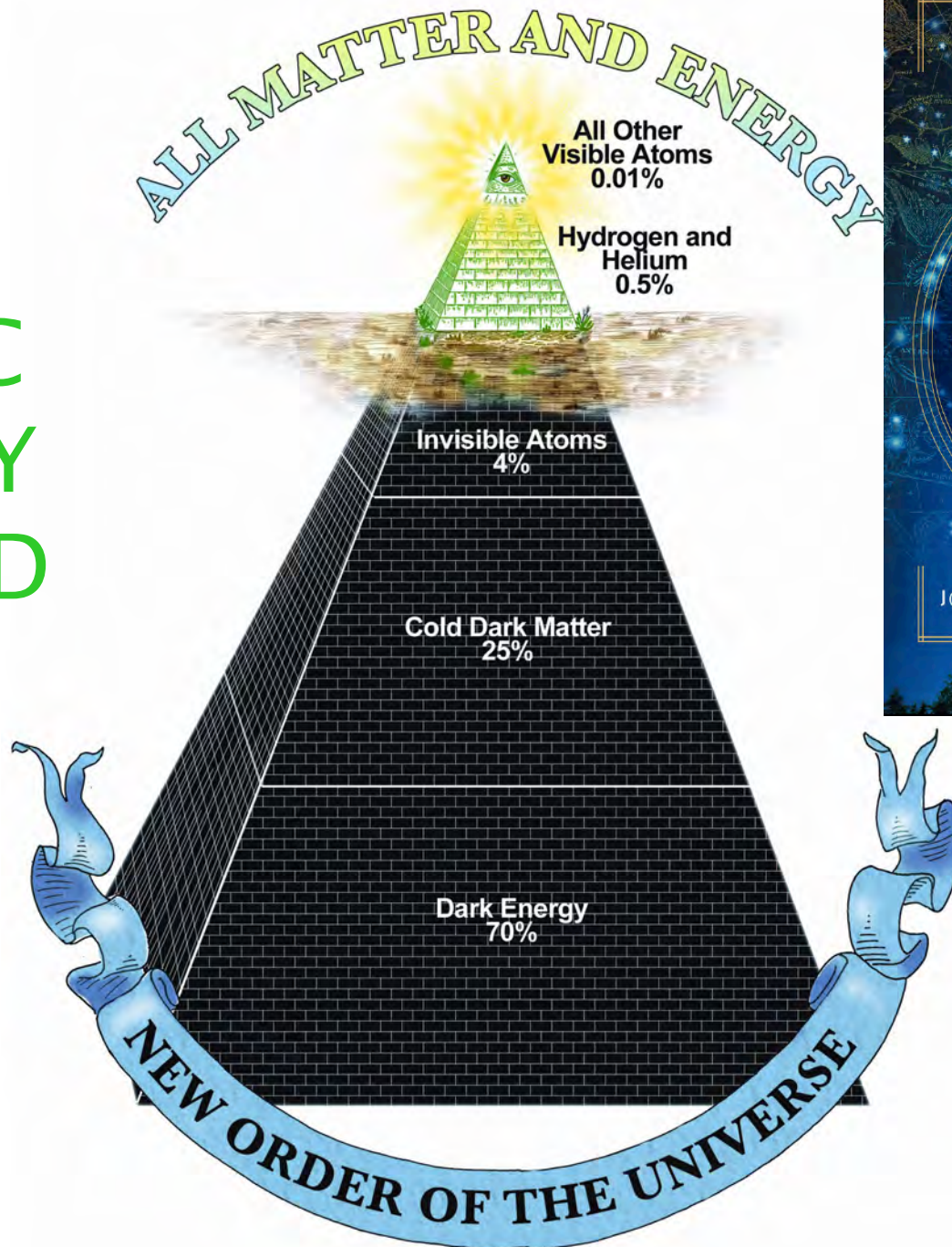
**Avishai Dekel (Hebrew U)
Matt Covington
(UCSC)Greg Novak
(UCSC)Christy Pierce**



stardust

stars

COSMIC DENSITY PYRAMID



<http://ViewfromtheCenter.com>

Stellar mass is mostly in galactic spheroids

spheroid:disk = 0.74:0.26 Fukugita & Peebles 2004

Stellar mass is mostly in galactic spheroids

spheroid:disk = 0.74:0.26 Fukugita & Peebles 2004

Generalized Merger Hypothesis

Mergers of **gas-rich** disks are the dominant process for forming spheroid and SMBH populations (following Toomre 1977)

This implies that mergers are the main mechanism for
most intense starbursts (ULIRGs)
bright quasar activity

Goals of Galaxy Interaction Simulations

Understand the amount of star formation due to galaxy mergers TJ Cox PhD thesis 04, Cox+05,06,07

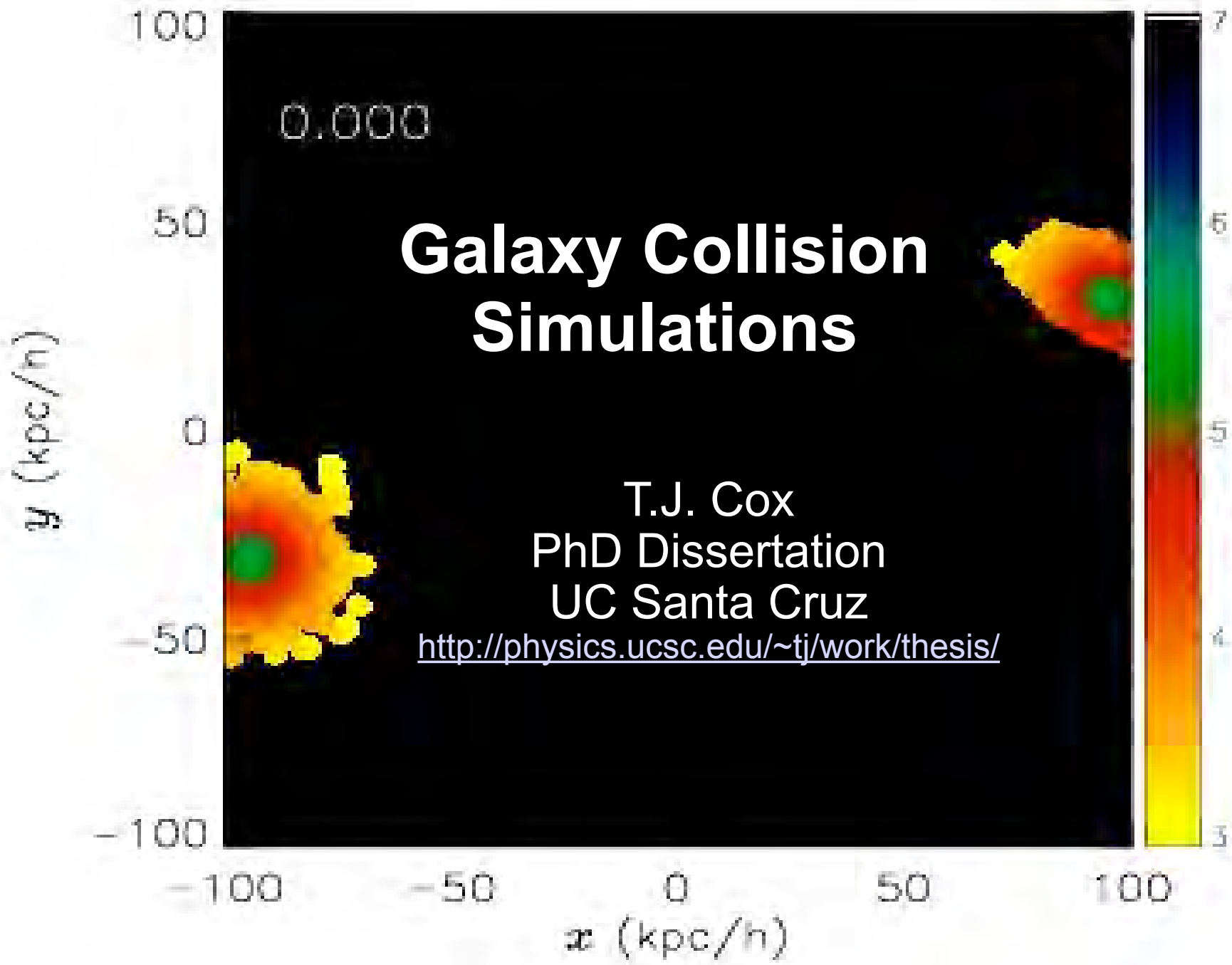
Study properties of merger remnants

DM/stellar/gas distributions Matt Covington+07

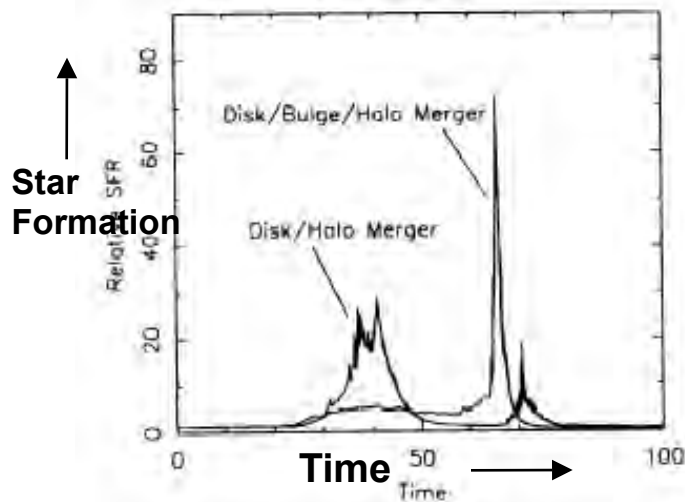
Angular momenta and kinematics Greg Novak

Predict appearance of interacting galaxies throughout merger, including dust scattering, absorption, and reradiation, and AGN P Jonsson PhD thesis 04, ApJ 06, MNRAS 06, in prep

Statistically compare to observations (DEEP2 and GOODS: ACS, Chandra, Spitzer, etc.) Jennifer Lotz, Piero Madau, and Primack 04, AJ; Lotz et al. 05, 06; Pierce et al. 06, Nandra et al. 06

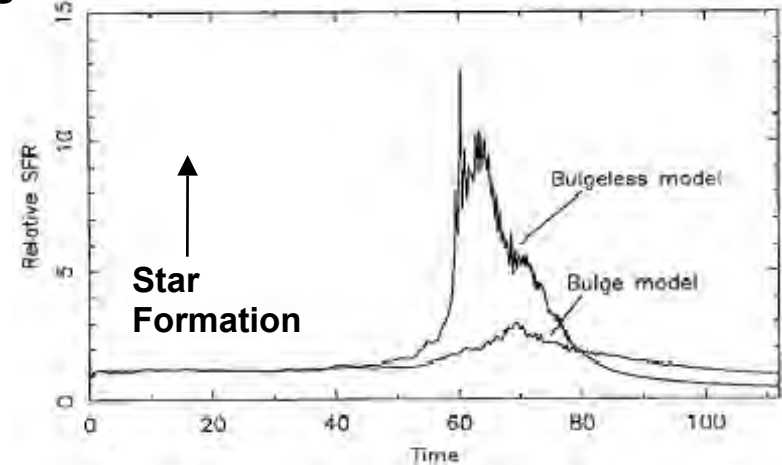


Numerical Simulations of Star Formation in Colliding Disk Galaxies: Earlier Work



- **Major mergers** (Mihos & Hernquist 1996, Springel 2000) (original disks are identical) generate significant bursts of star formation consuming $\sim 80\%$ of the original gas mass.
- Internal structure of progenitor disk galaxy (i.e. the presence of a bulge or not) dictates when the gas is funneled to the center and turned into stars.

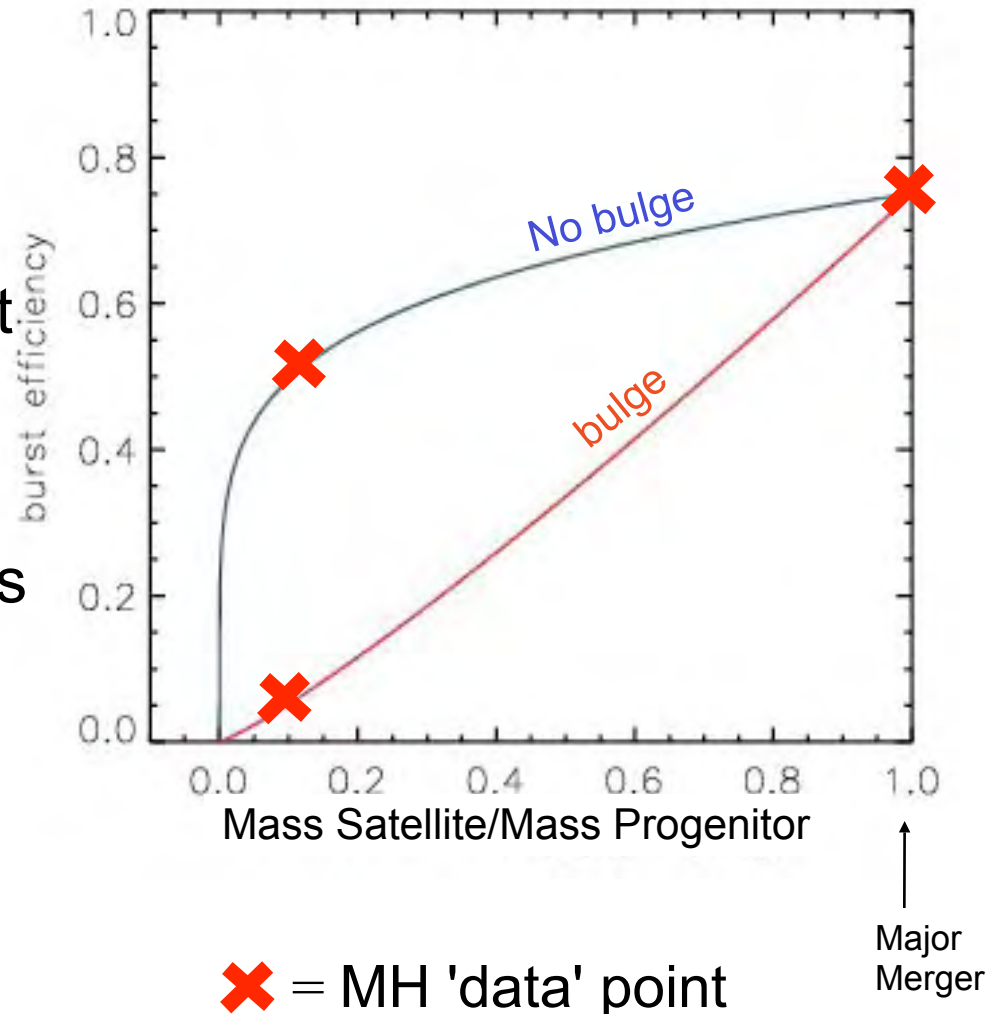
- **Minor mergers** (Mihos & Hernquist 1994) (satellite galaxy is 10% of the original disk mass) generate significant bursts of star formation only when there is no bulge in progenitor disk galaxy.



→ **NOTE:** These simulations used a version of SPH which has been shown not to conserve entropy (Springel & Hernquist 2002).

Parameterizing Starbursts

Based upon the results of Mihos & Hernquist (the 3 'data' points), Somerville, Primack & Faber (2001, SPF01) estimated the burst efficiency (amount of gas converted to stars due to the galaxy merger) as a function of the merger mass ratio. A motivation of the present work is to improve the statistics and understanding of mergers.



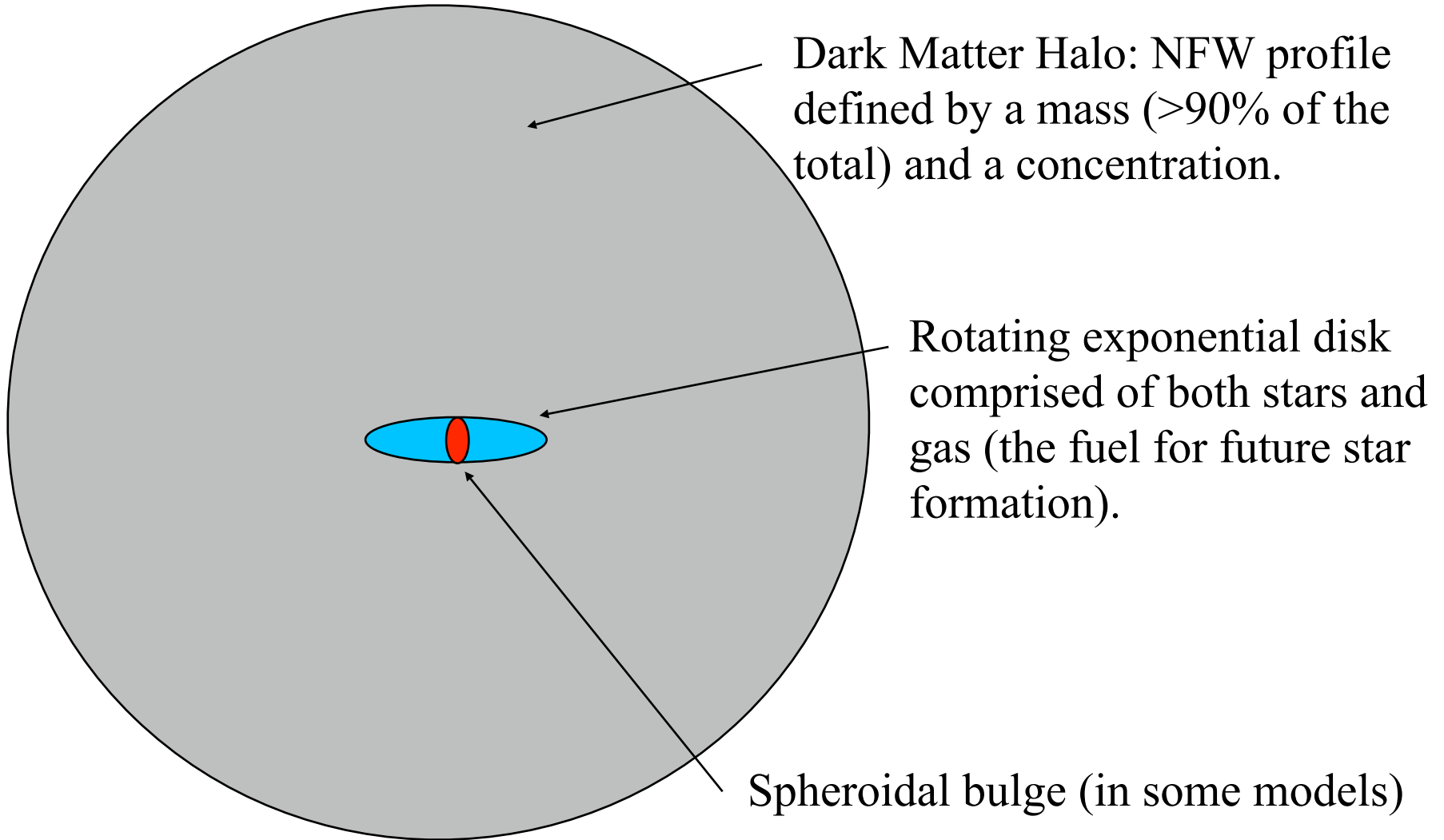
Our New Work

In order to investigate galaxy mergers (and interactions) we build observationally motivated N-body realizations of compound galaxies and simulate their merger using the SPH code GADGET (Springel, Yoshida & White 2000, Springel 2005). These simulations include:

- An improved version of smooth particle hydrodynamics (SPH) which explicitly conserves both energy and entropy (Springel & Hernquist 2002).
- The radiative cooling of gas
- Star formation: $\rho_{\text{sfr}} \sim \rho_{\text{gas}} / \tau_{\text{dyn}}$ for $(\rho_{\text{gas}} > \rho_{\text{threshold}})$
- Metal Enrichment
- Stellar Feedback

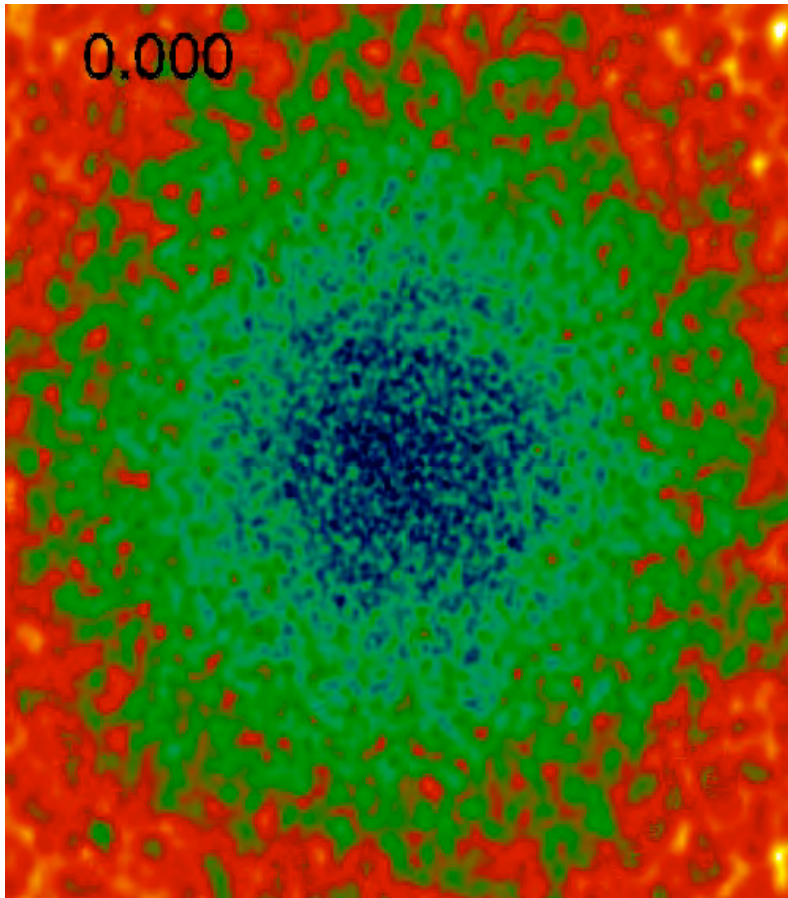
* Our simulations contain $\geq 170,000$ particles / big galaxy and the resolution is typically ~ 100 pc. (Tested up to 1.7×10^6 particles.)

Initial Conditions

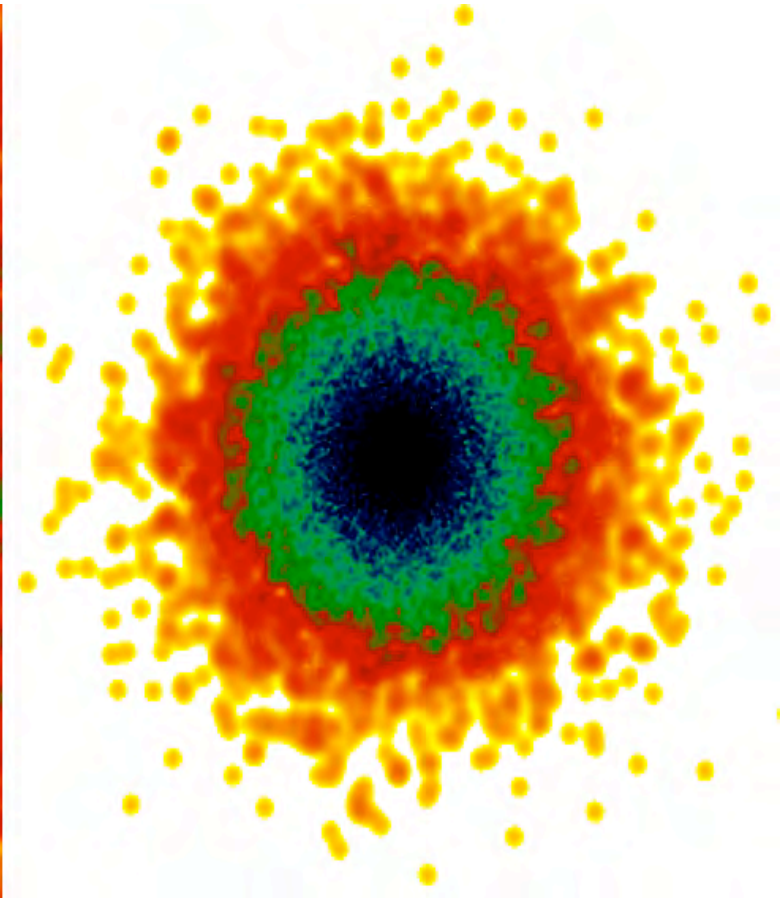


Stable Disk

100 kpc



Gas



Star

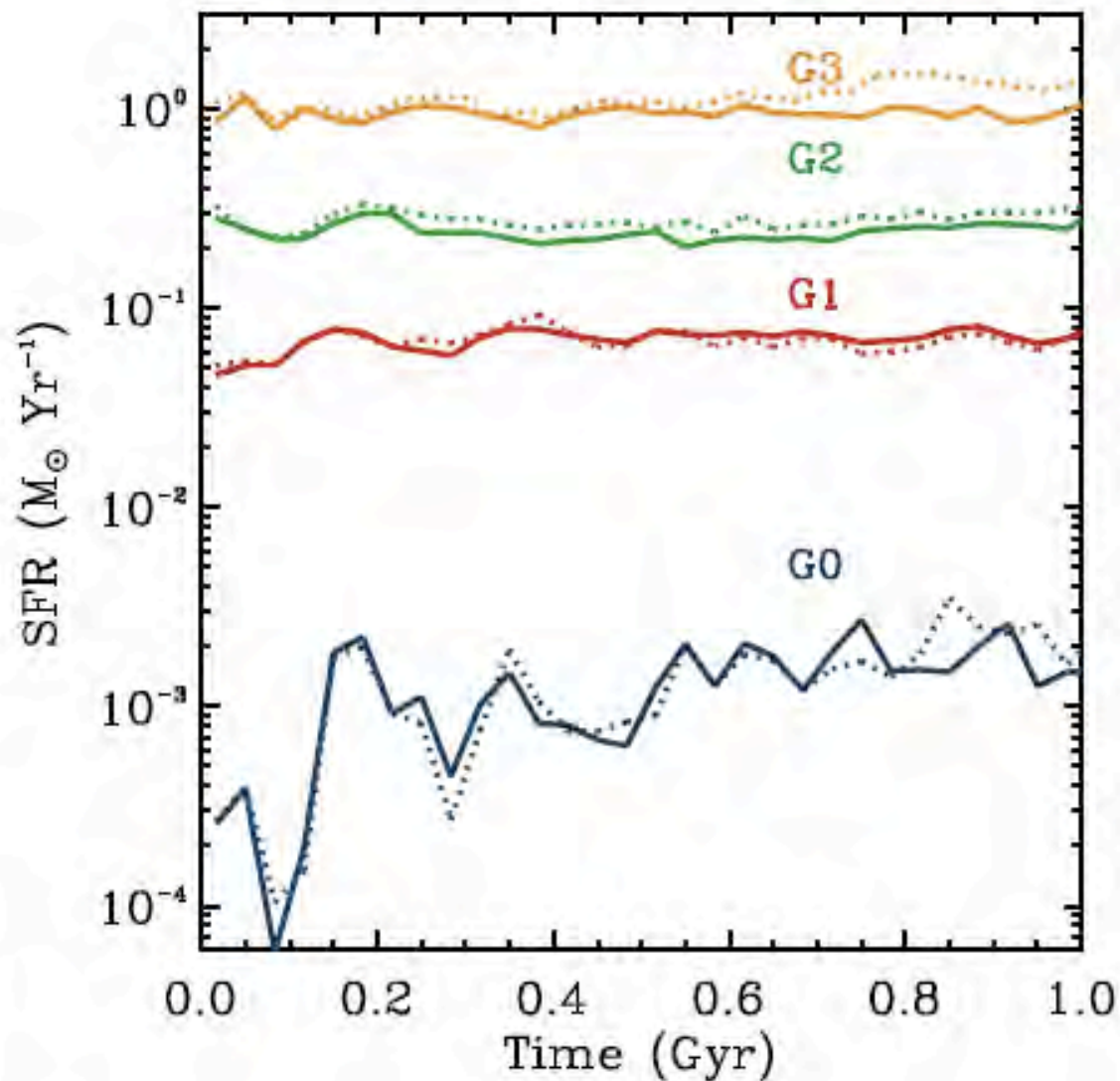


Figure 2. Star formation for our isolated galaxy models G3, G2, G1 and G0. Each model has been run with two separate feedback models and both star-formation histories are shown, n2med with a solid line and n0med with a dotted line.

	G3	G2	G1	G0
M_* ($10^{10} M_\odot$)	5.0	1.5	0.5	0.1
R_{50} (kpc)	3.86	2.88	2.35	1.83
Total Mass, M_{vir} ($10^{10} M_\odot$)	116.0	51.0	20.0	5.0
Concentration, $c=R_{\text{vir}}/r_s$	6	9	12	14
Spin Parameter, λ	0.05	0.05	0.05	0.05
Disk Mass, M_{disk} ($10^{10} M_\odot$)	4.11	1.35	0.47	0.098
Disk Mass Fraction, m_d	0.035	0.026	0.024	0.019
Disk Scale Length, R_d (kpc)	2.85	1.91	1.48	1.12
Disk Scale Height, z_0 (kpc)	0.40	0.38	0.30	0.22
Disk Spin Fraction, j_d	0.015	0.010	0.010	0.010
Bulge Mass, M_{bulge} ($10^9 M_\odot$)	8.9	1.5	0.3	0.02
Bulge-to-disk ratio, B/D	0.22	0.11	0.06	0.02
Bulge Mass Fraction, m_b	0.008	0.003	0.002	<0.001
Bulge Radial Scale Length, R_b (kpc)	0.37	0.26	0.20	0.15
Gas Mass, M_{gas} ($10^{10} M_\odot$)	1.22	0.48	0.20	0.06
Gas Mass Fraction, m_g	0.011	0.009	0.010	0.012
Gas Fraction, f	0.196	0.242	0.286	0.375
Gas Scale Multiplier, α	3.0	3.0	3.0	3.0
Gas Spin Fraction, j_g	0.012	0.010	0.013	0.019
N	240,000	150,000	95,000	51,000
N_{dm}	120,000	80,000	50,000	30,000
N_{gas}	50,000	30,000	20,000	10,000
N_{disk}	50,000	30,000	20,000	10,000
N_{bulge}	10,000	10,000	5,000	1,000

Major and minor mergers...

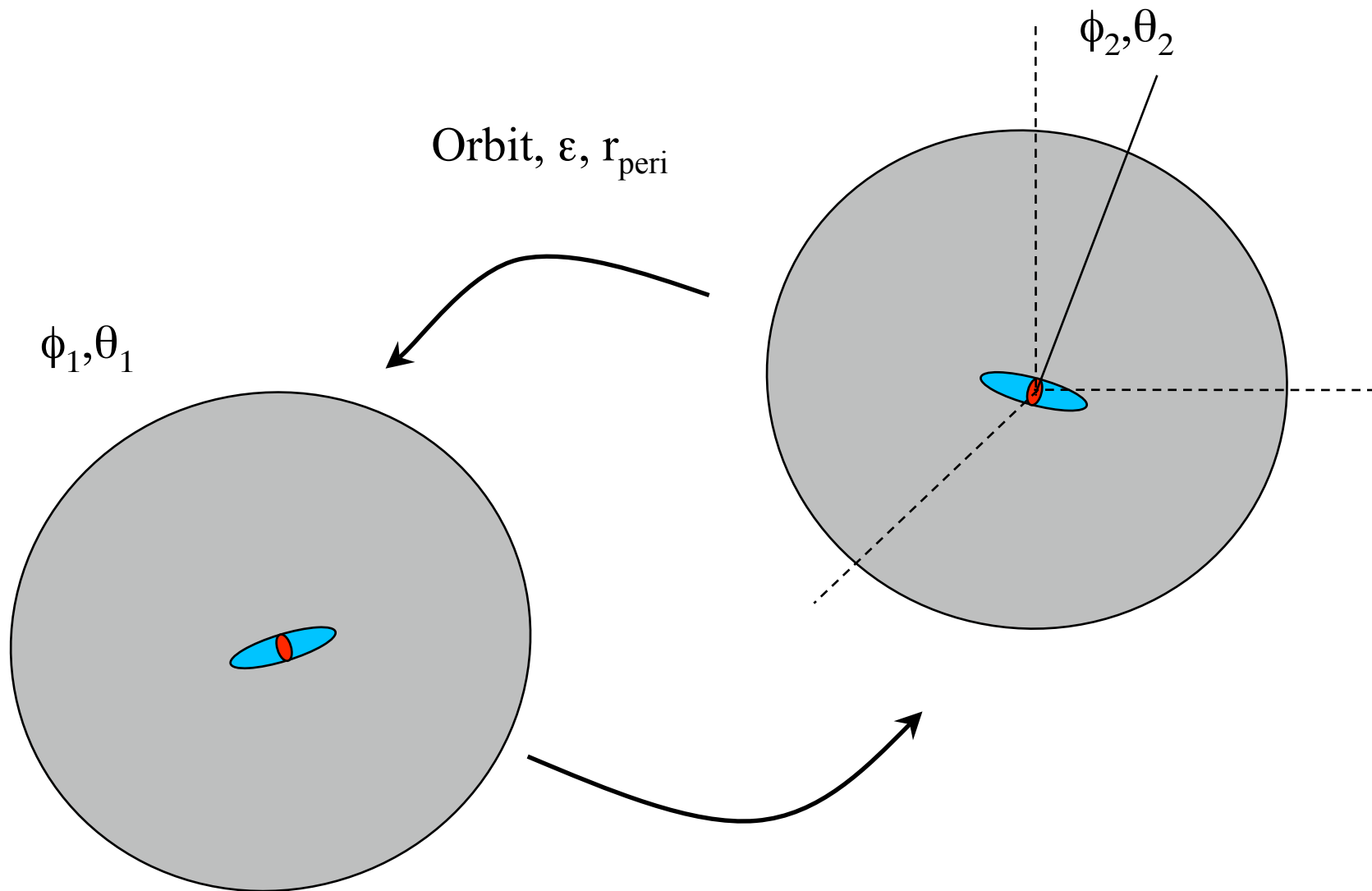
Merger Mass Ratios

Primary	Satellite	Total	Stellar	Baryonic
G3	G3	1:1	1:1	1:1
G3	G2	2.3:1	3.3:1	3.1:1
G3	G1	5.8:1	10.0:1	8.9:1
G3	G0	22.7:1	50.0:1	38.9:1
G2	G2	1:1	1:1	1:1
G2	G1	2.6:1	3.0:1	2.8:1
G2	G0	10.0:1	15.0:1	12.4:1
G1	G1	1:1	1:1	1:1
G1	G0	3.9:1	5.0:1	4.4:1
G0	G0	1:1	1:1	1:1

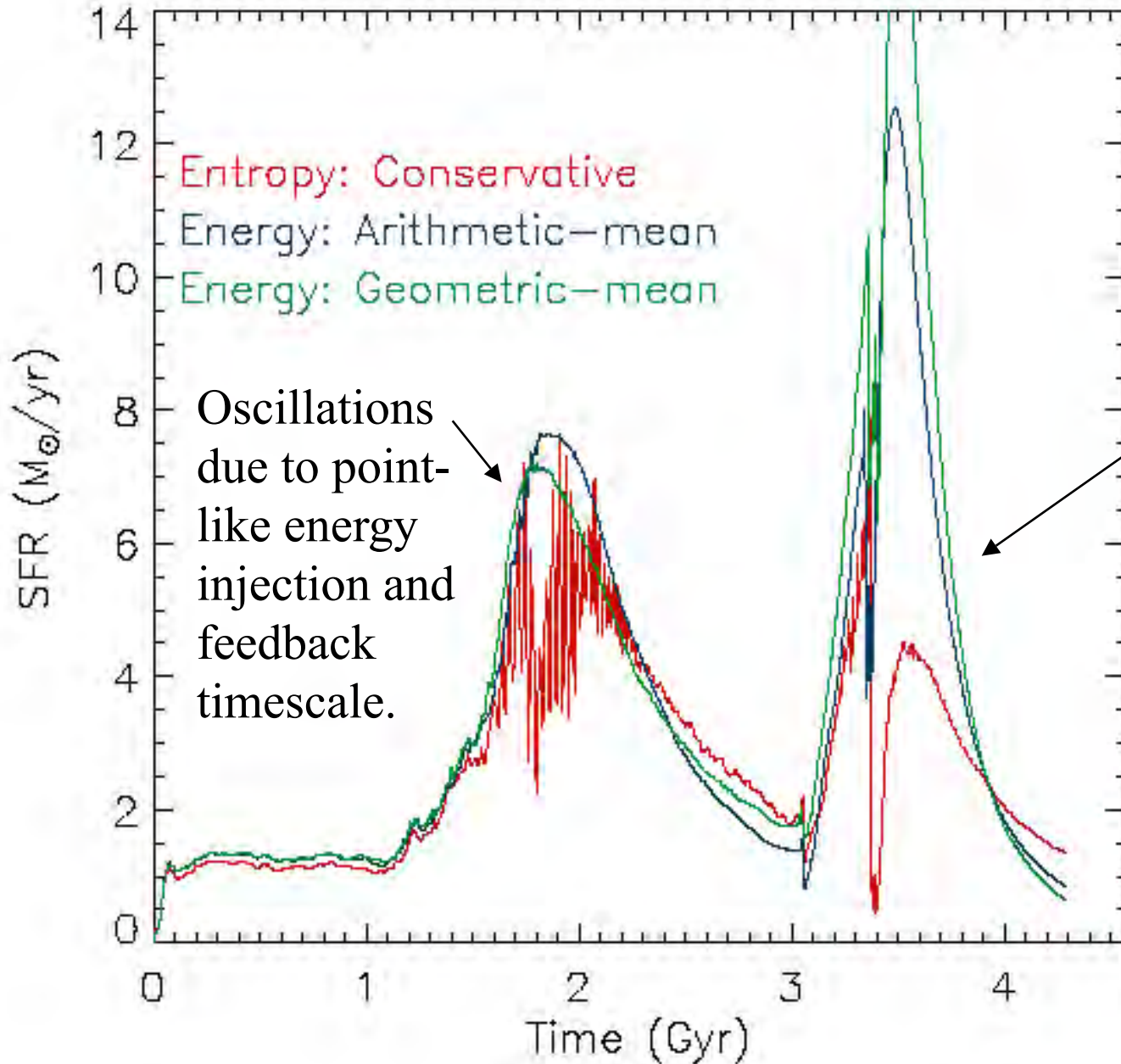
G3G3: Major merger between two G3's

G3G1: Minor merger between G3 and smaller G1

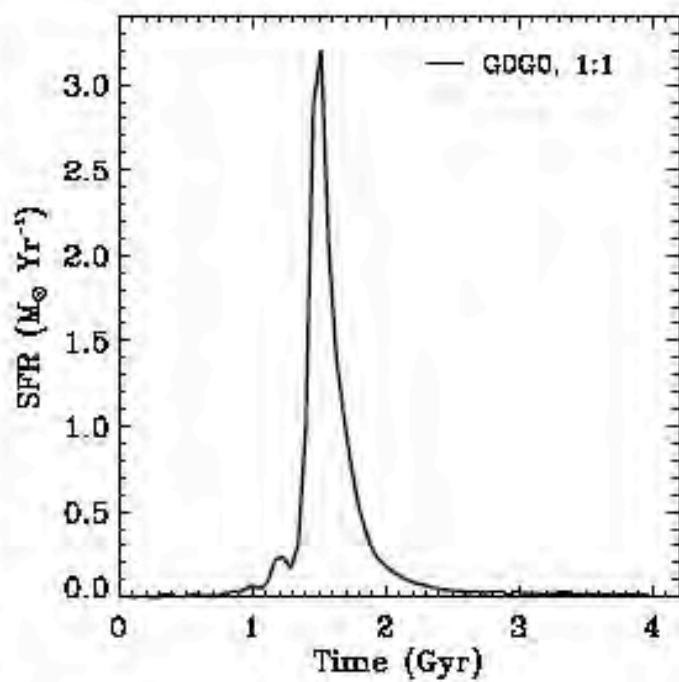
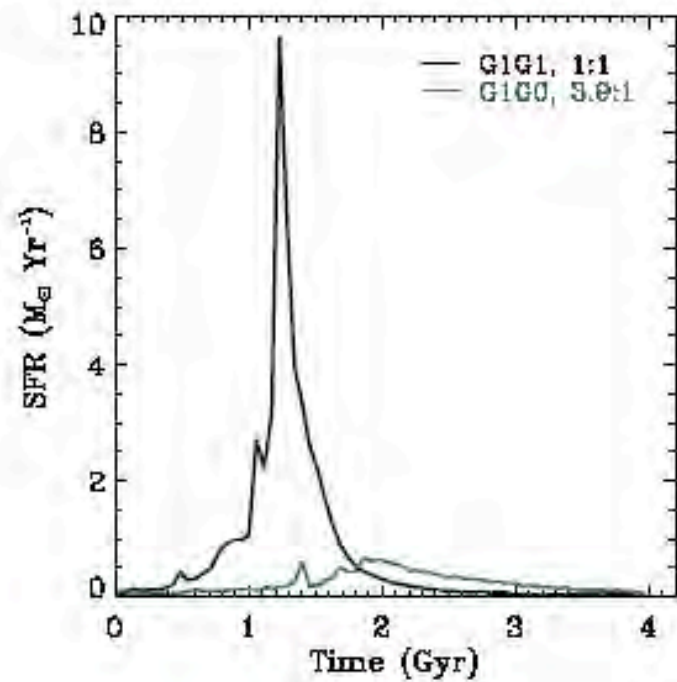
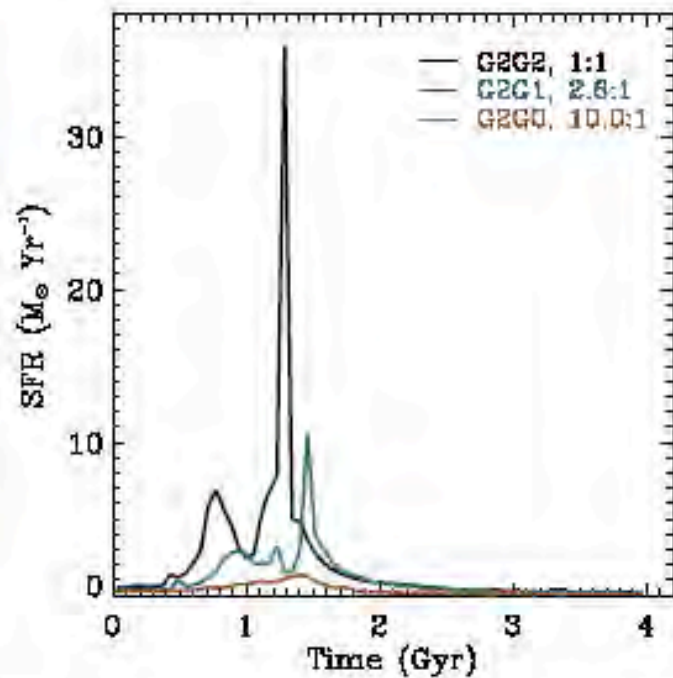
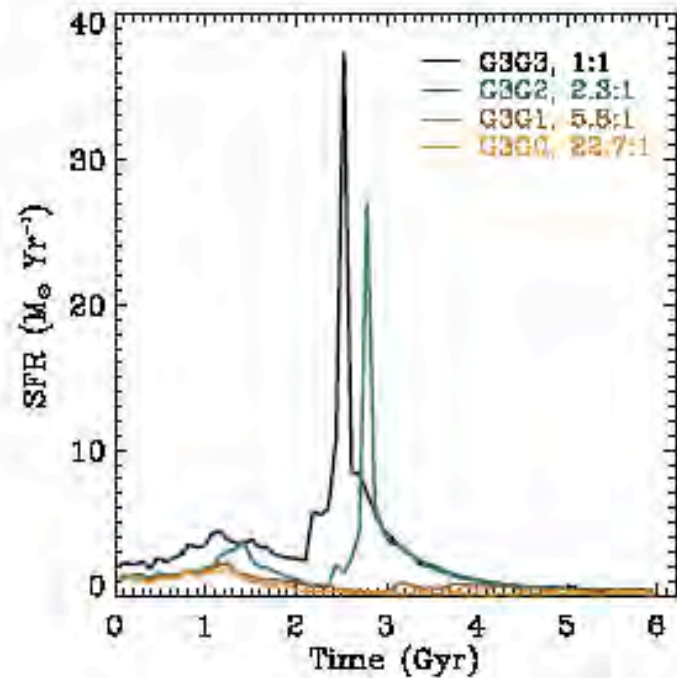
Now Let's Merge Two Disks



SPH & Star Formation



Half as much star formation during final merger with entropy-conserving SPH.



Projected Gas Density
in the orbital plane

Projected Stellar Density
in the orbital plane

left: Projected gas density
right: Projected stellar density
XY, the orbital plane

G Model Minor Merger

Run: G3G2r-u3

T.J. Cox & Patrik Jonsson, UC Santa Cruz

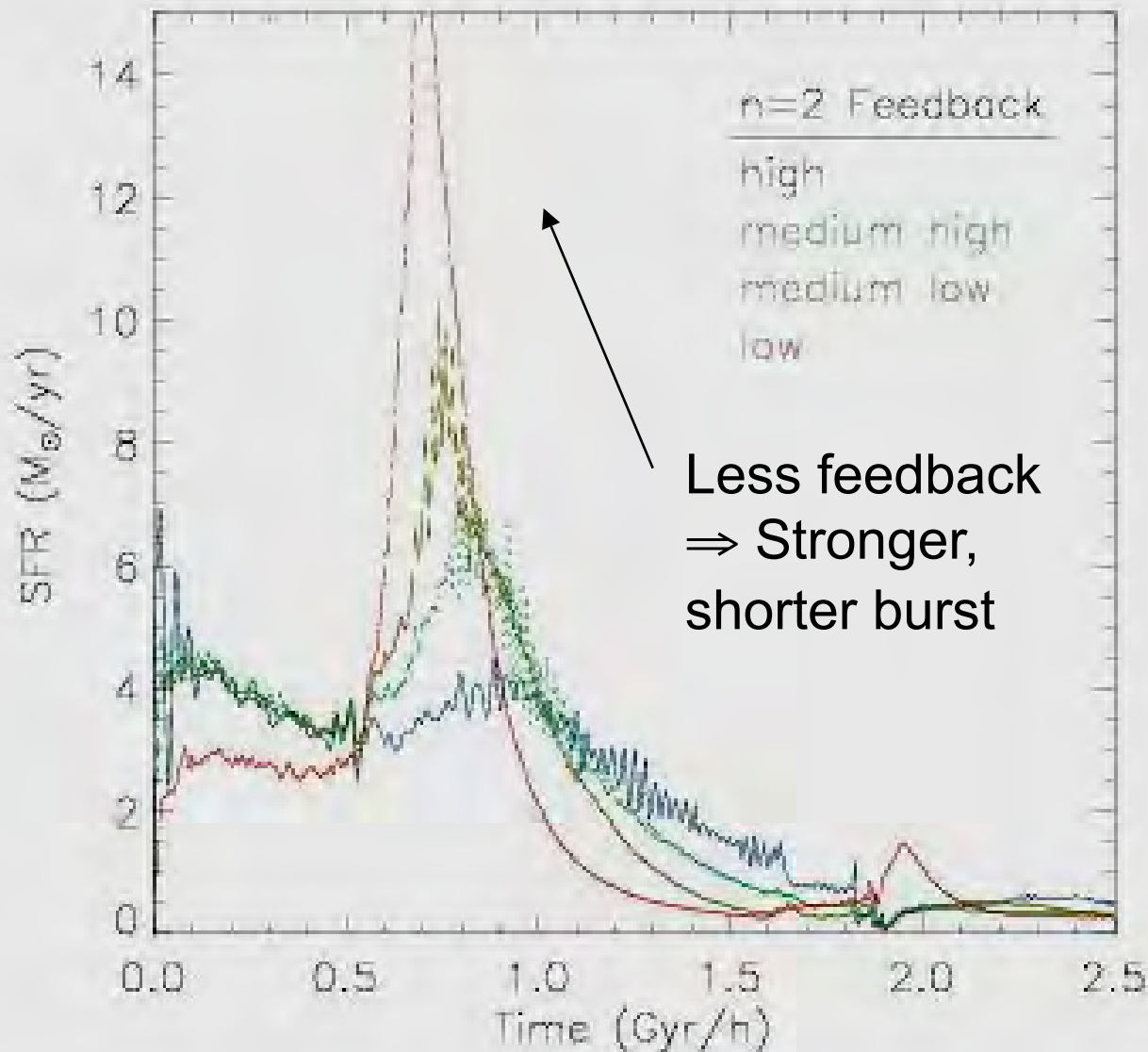
UC Santa Cruz, 2004

G3G2r: 1:3 retrograde merger

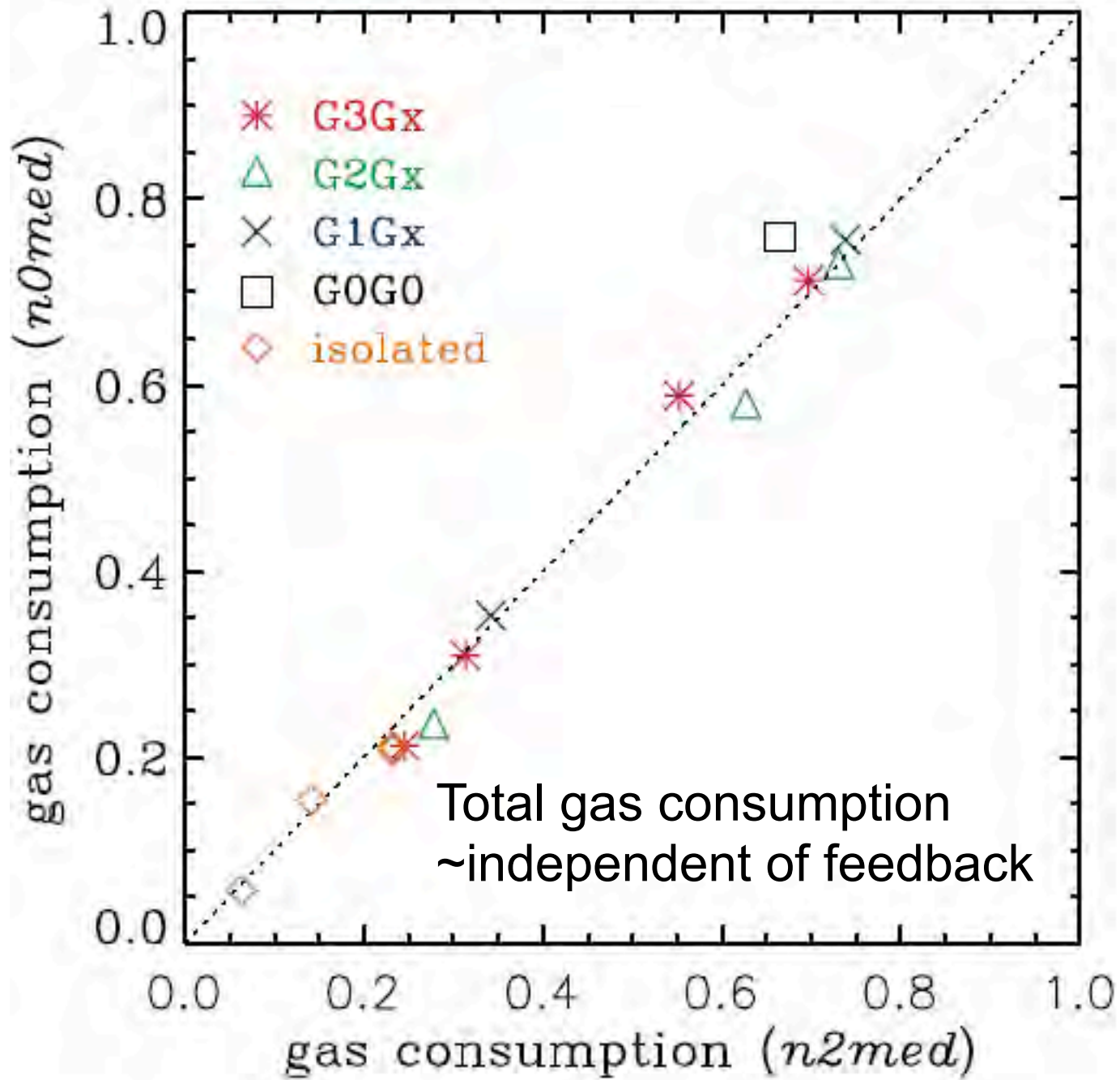
Movie at:

<http://physics.ucsc.edu/~tj/work/movies/>

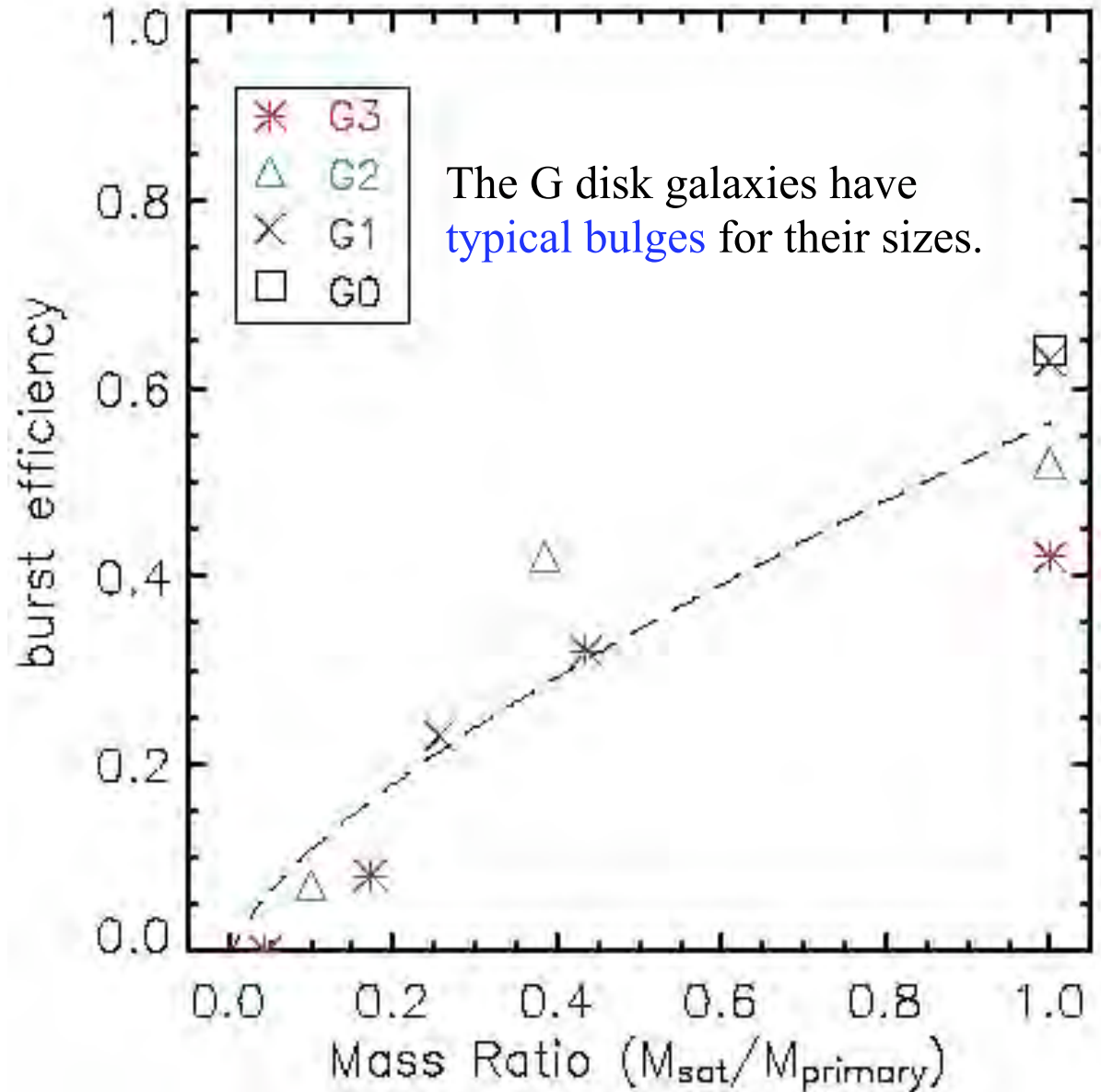
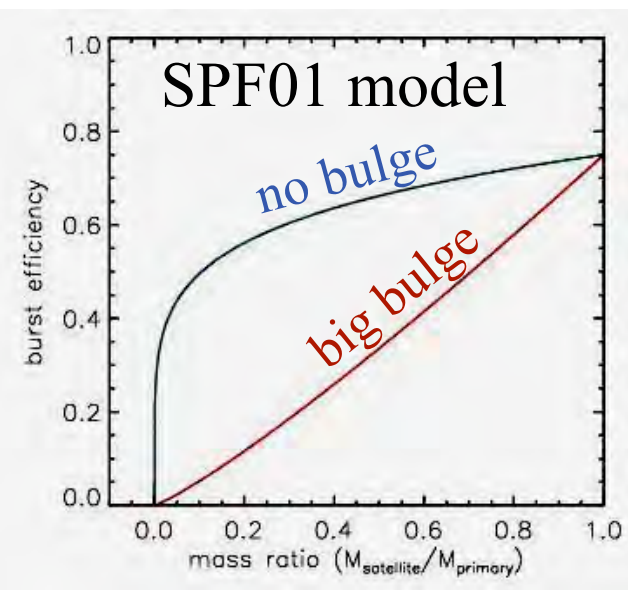
SFR vs. Free Parameters



While SF/Fb parameters are fixed to make star formation fall on Kennicutt (1998), we can still get a range of burst strengths and durations.



Burst Efficiency



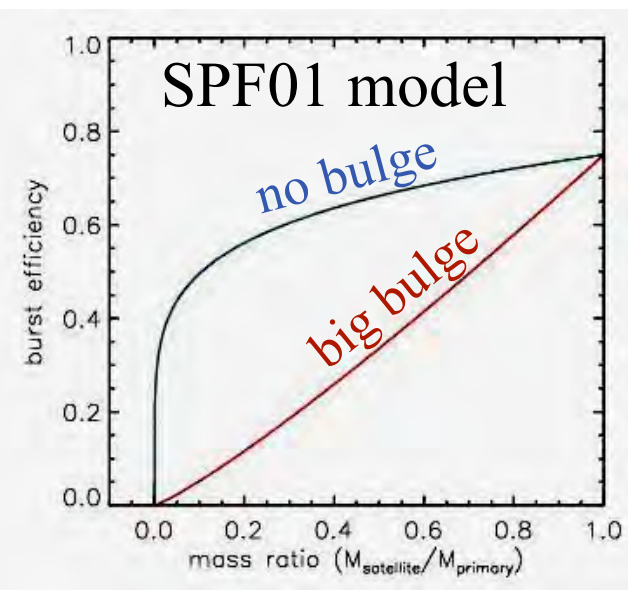
The quiescent star formation has been subtracted.

$$e = e_{1:1} \left(\frac{M_{\text{sat}}}{M_{\text{primary}}} \right)^\gamma$$

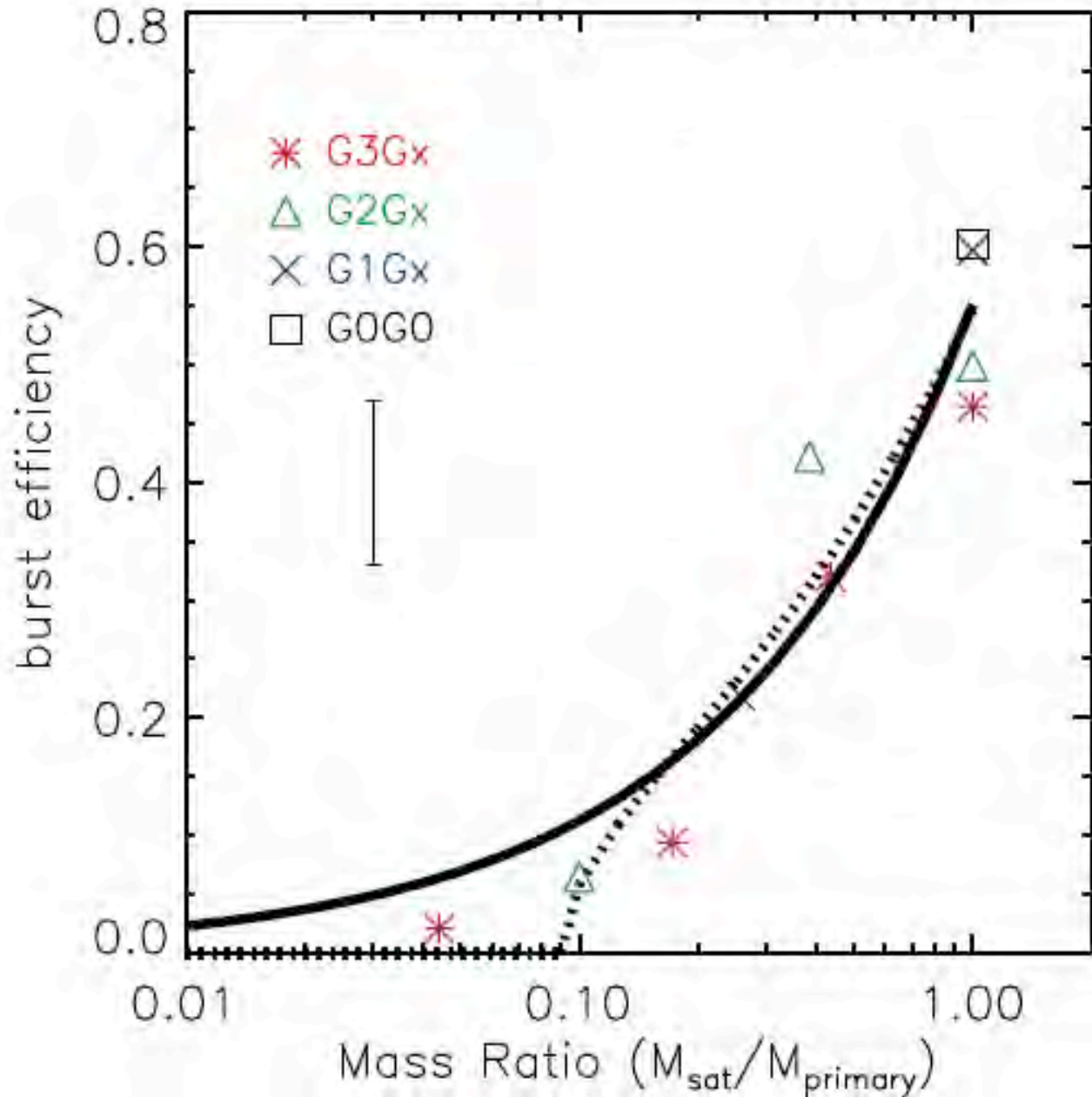
$$e_{1:1} = 0.56$$

$$\gamma = 0.7$$

Burst Efficiency

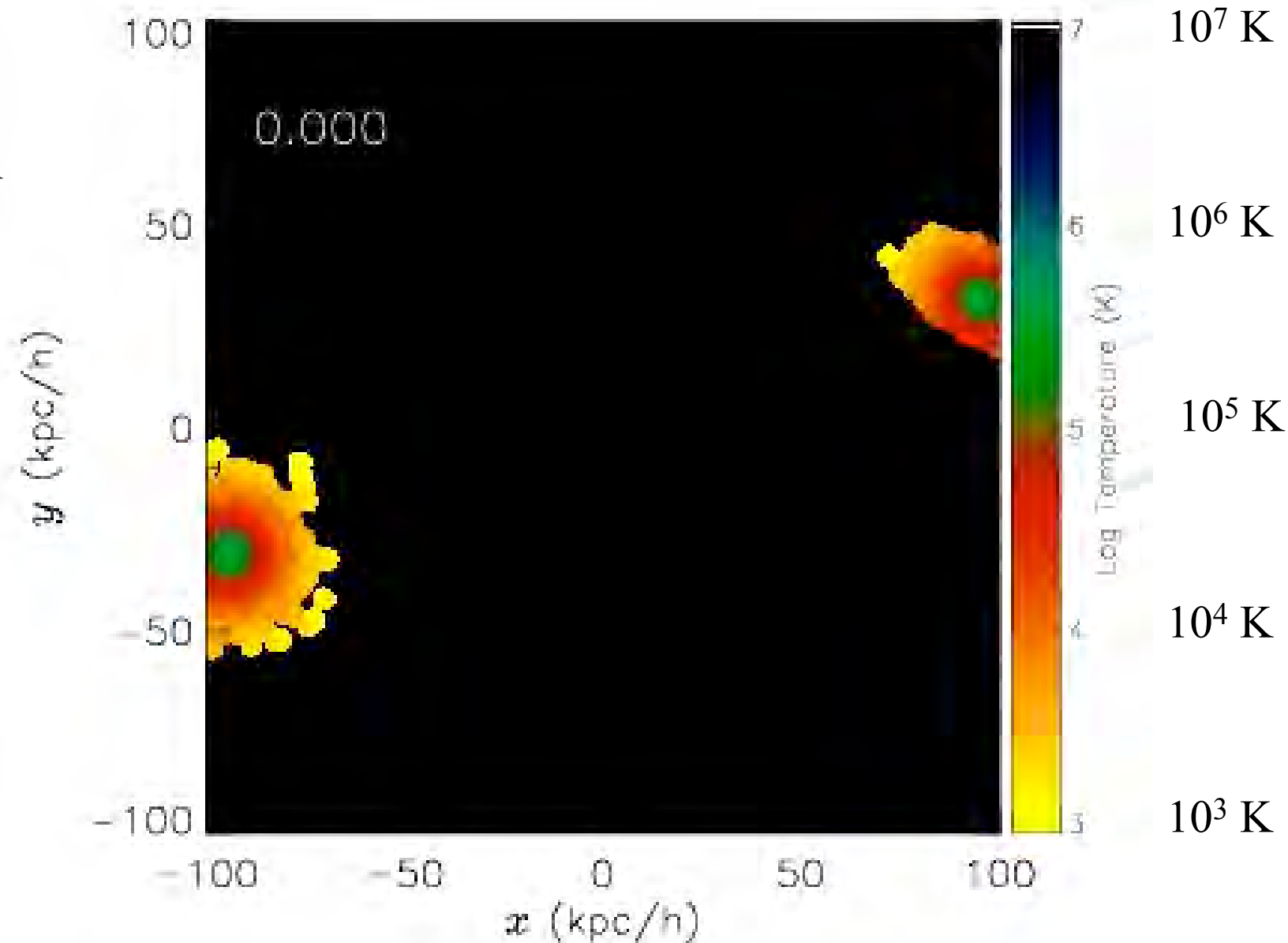


The quiescent star formation has been subtracted.



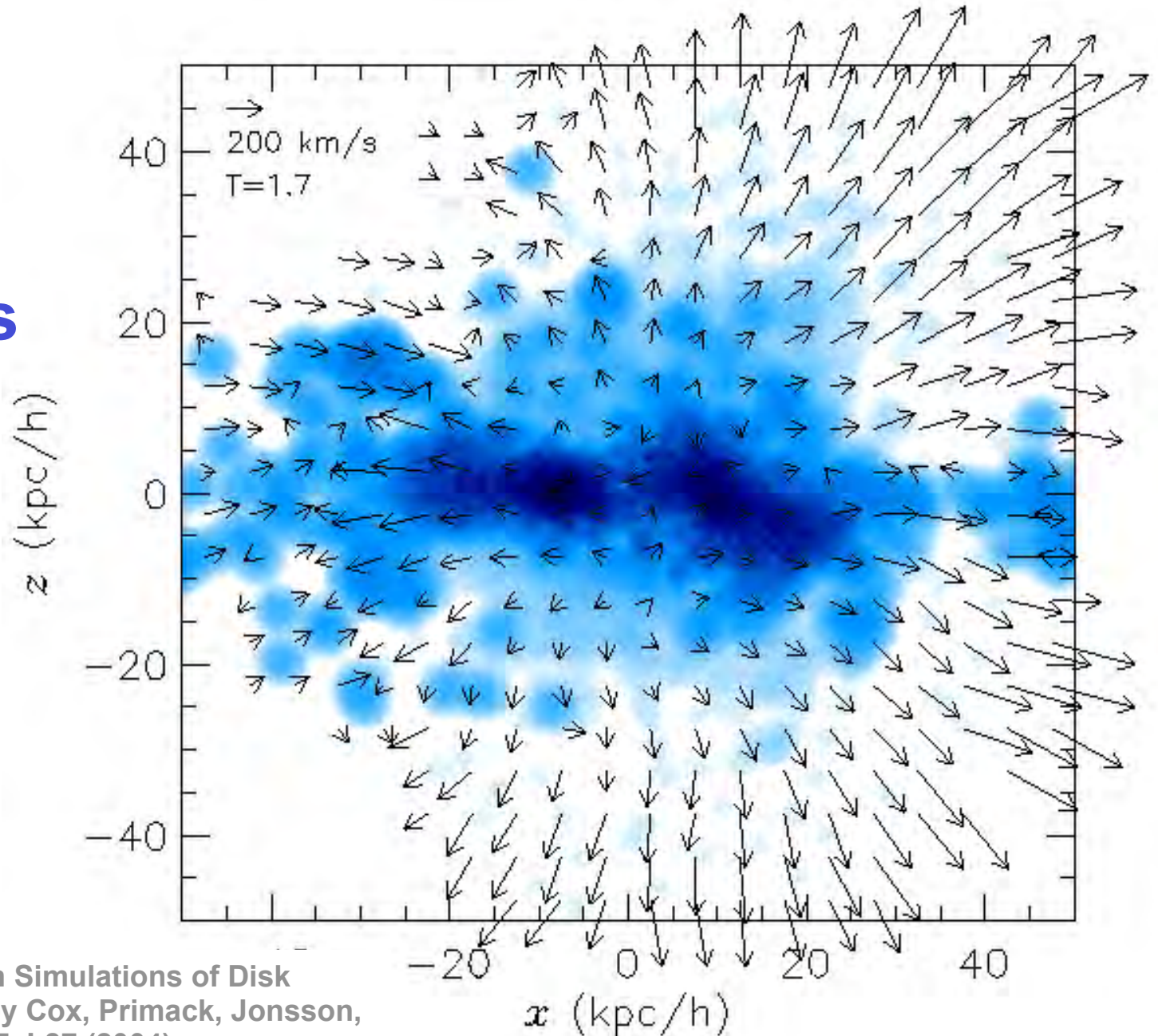
Gas Temperature during Major Merger

7 kpc
slice
through
orbital
plane



Gas velocity field on color gas density map

7 kpc slice through plane perpendicular to orbital plane



Generating Hot Gas in Simulations of Disk Galaxy Interactions, by Cox, Primack, Jonsson, & Somerville, ApJ, 607, L87 (2004).

Spatial, velocity, and angular momentum distribution of dark matter, stars, and gas in merger remnants:

Comparison with Planetary Nebulae and Globular Clusters –
“Dark-Matter Haloes in Elliptical Galaxies: Lost and Found”
Avishai Dekel et al., *Nature*, 437, 707 (2005)

Semi-analytic models of merger remnant properties (e.g., M^* , $r_{1/2}$, σ_v , gas) – in progress by UCSC grad student **Matt Covington** working with Dekel and Primack. **Radius and velocity dispersion predicted. Massive major mergers lie in fundamental plane, lower mass disky remnants do not.**

Comparison with PNe and SAURON, and shapes of stellar spheroid and dark matter halos of merger remnants – in progress by UCSC grad student **Greg Novak** working with Dekel, Faber, and Primack.

Comparison with Planetary Nebulae and Globular Clusters

“Dark-Matter Haloes in Elliptical Galaxies: Lost and Found” -- Dekel et al., *Nature*, 437, 707 (2005)

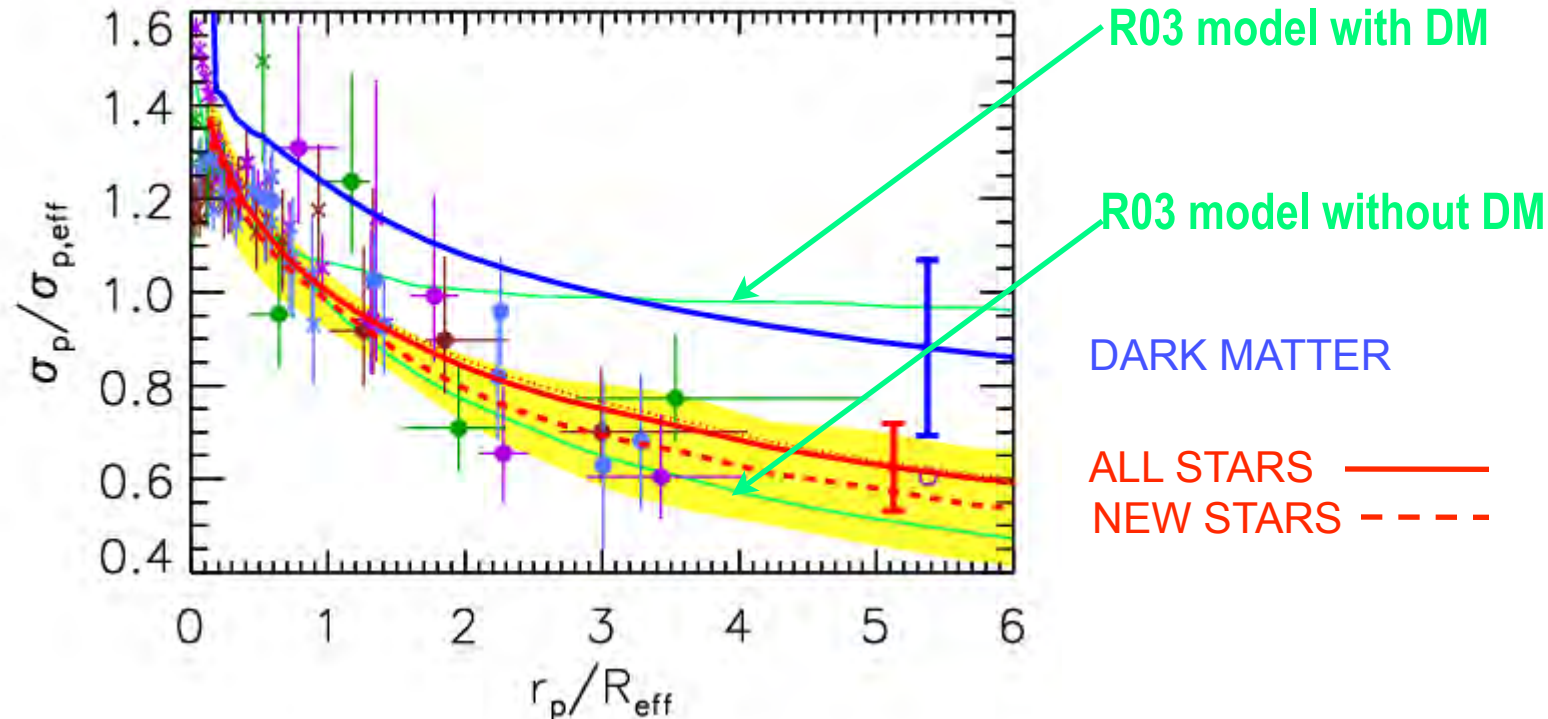
We show what's wrong with the conclusions drawn by

Romanowsky, Douglas, Arnaboldi, Kuijken, Merrifield, Napolitano, Capaccio li, & Freeman, “**A Dearth of Dark Matter in Ordinary Elliptical Galaxies**” *Science* **301**, 1696 (2003)

Abstract: The kinematics of the outer parts of three intermediate-luminosity elliptical galaxies were studied with the Planetary Nebula Spectrograph. The **galaxies' velocity-dispersion profiles were found to decline with the radius, and dynamical modeling of the data indicates the presence of little if any dark matter in these galaxies' halos.** This unexpected result conflicts with findings in other galaxy types and poses a challenge to current galaxy formation theories.

Note that more recent X-ray and Globular Cluster data imply massive dark matter halos in at least two of these galaxies. They thus conflict with this claim and are consistent with our simulations.

Comparison with Planetary Nebulae and Globular Clusters – “Dark-Matter Haloes in Elliptical Galaxies: Lost and Found” Dekel et al., *Nature*, 707, 437 (2005) astro-ph/0501622



Projected velocity dispersion profiles: simulated galaxies versus observations. Ten major merger remnants are viewed from three orthogonal directions and the 60 profiles are stacked such that the stellar curves (“old”+“new”) match at R_{eff} . Dark matter (blue) versus stars (red), divided into “old” (dotted) and “new” (dashed). The < 3 Gyr “new” stars mimic the observed PNs. The shaded areas and thick bars mark 1σ scatter, partly due to triaxiality. The Romanowsky galaxies are marked green (821), violet (3379), brown (4494) and blue (4697). The surface densities shown for NGC 3379 and 4697 almost coincide with the simulated profile. Green lines refer to the R03 models with (upper) and without (lower) dark matter.

MERGER REMNANTS LIE IN THE FUNDAMENTAL PLANE

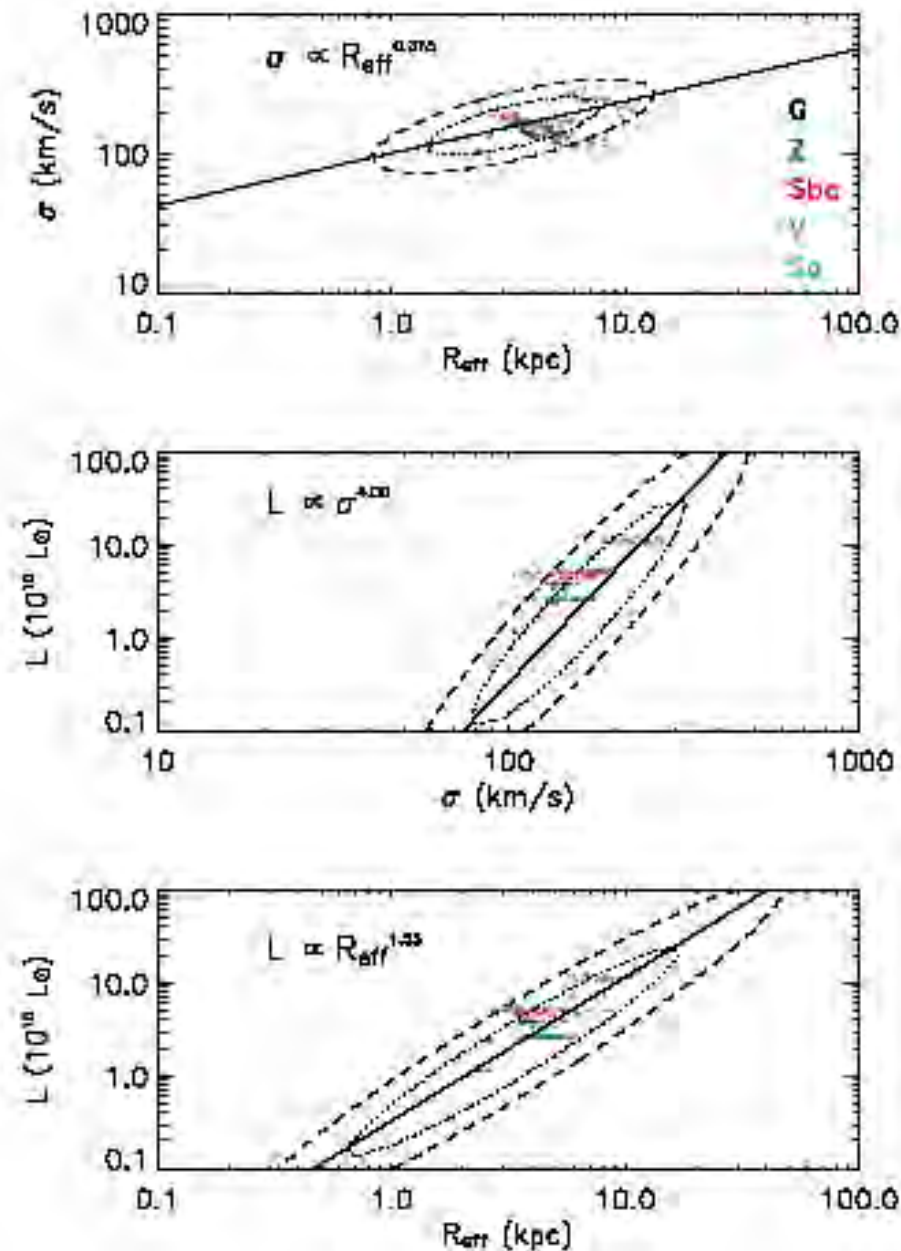


Figure 11. The global structure properties of the simulated merger remnants (symbols, colored by the merger type) in comparison with the Fundamental Plane distribution of elliptical galaxies in SDSS (1 and 2 contours). The dispersion velocity is measured in the central regions. The luminosity is derived from the stellar mass assuming an effective $M/L = 3$.

From Supplementary Information online with Nature article, also at [astro-ph/0501622](https://arxiv.org/abs/astro-ph/0501622). Based on work by [Matt Covington](#) with Avishai Dekel and Joel Primack. See also Robertson et al. 2005.

A Physical Model for Predicting the Properties of Merger Remnants

We might expect that a more energetic encounter will cause increased tidal stripping and puff up the remnant.

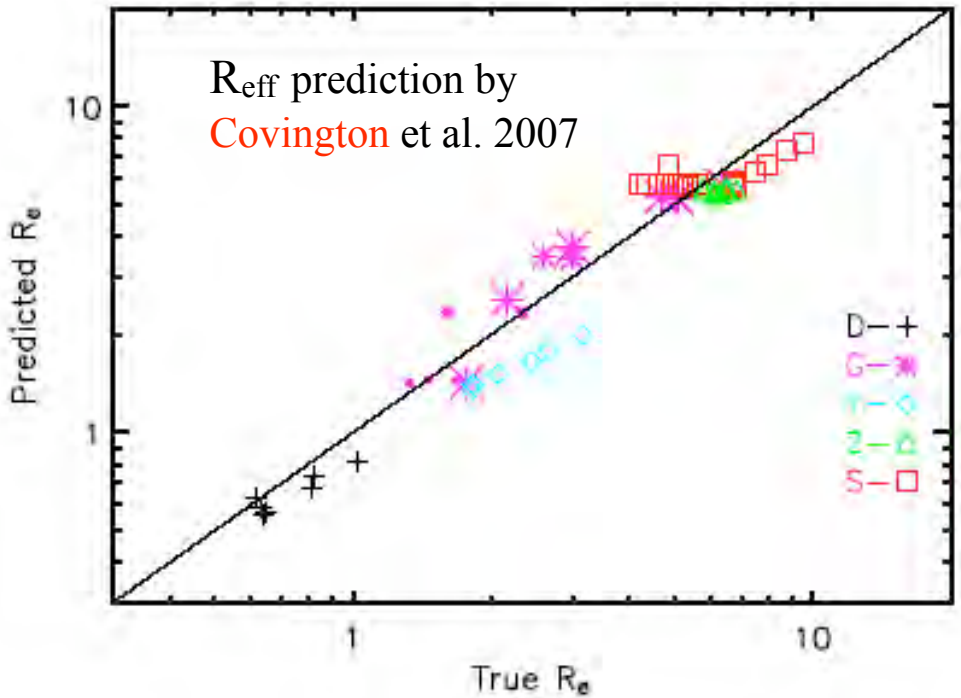
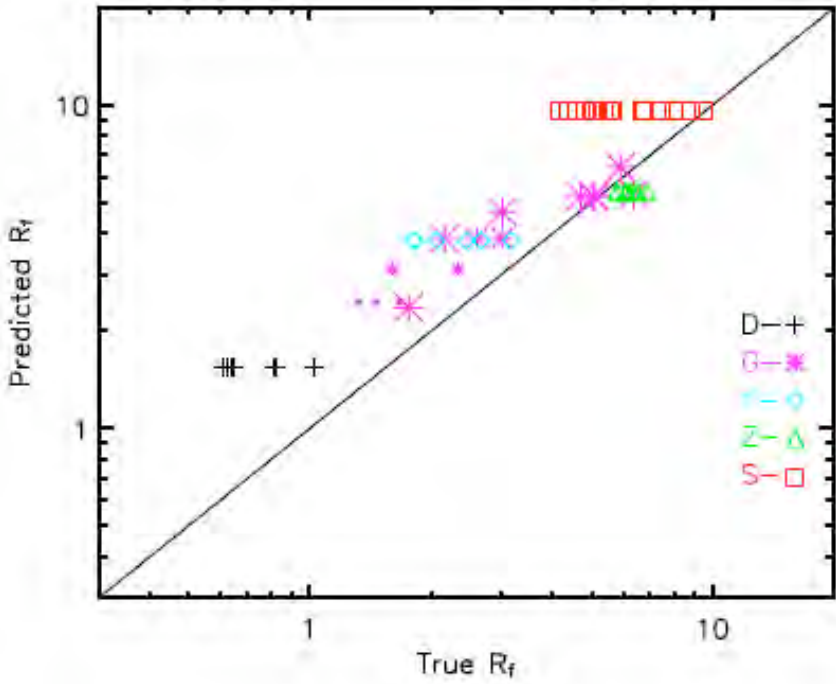
NO! For our simulations, more **energetic encounters** create more **compact remnants**.

Why? Dissipative effects cause more energetic encounters to result in smaller remnants.

Impulse provides a measure of merger “violence.” The greater the impulse, the more the gas is disturbed, therefore the more it can radiate and form stars.

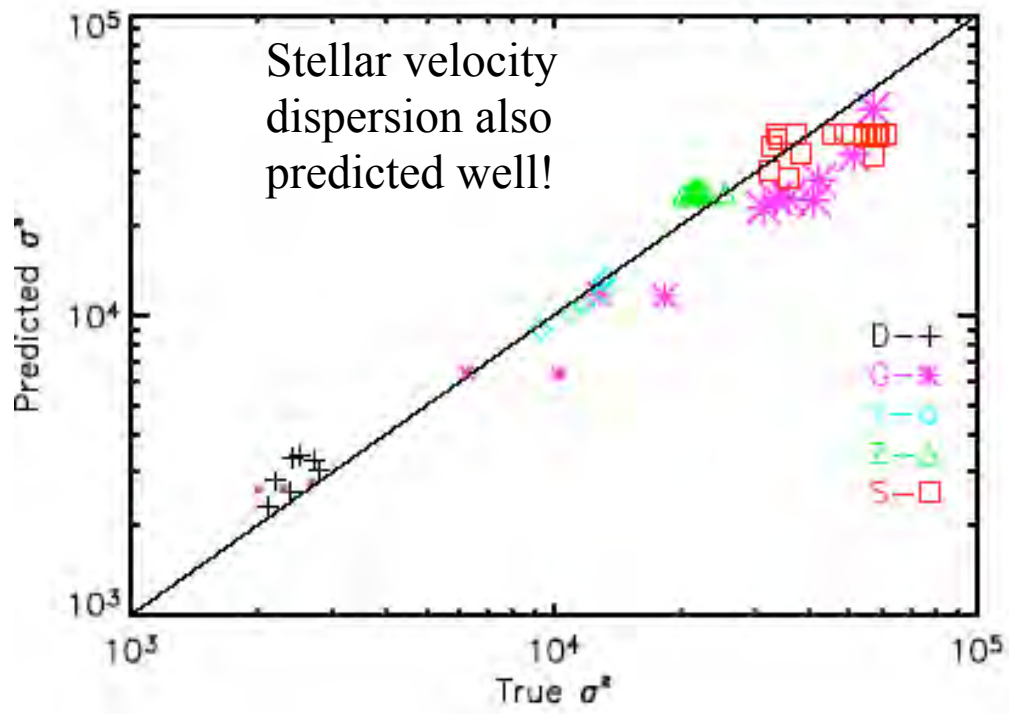
A number of physical mechanisms conspire to make this so (e.g. greater tidal effects, lower angular momentum, and more gas disk overlap).

Matt Covington, Cox, Dekel, & Primack 2007



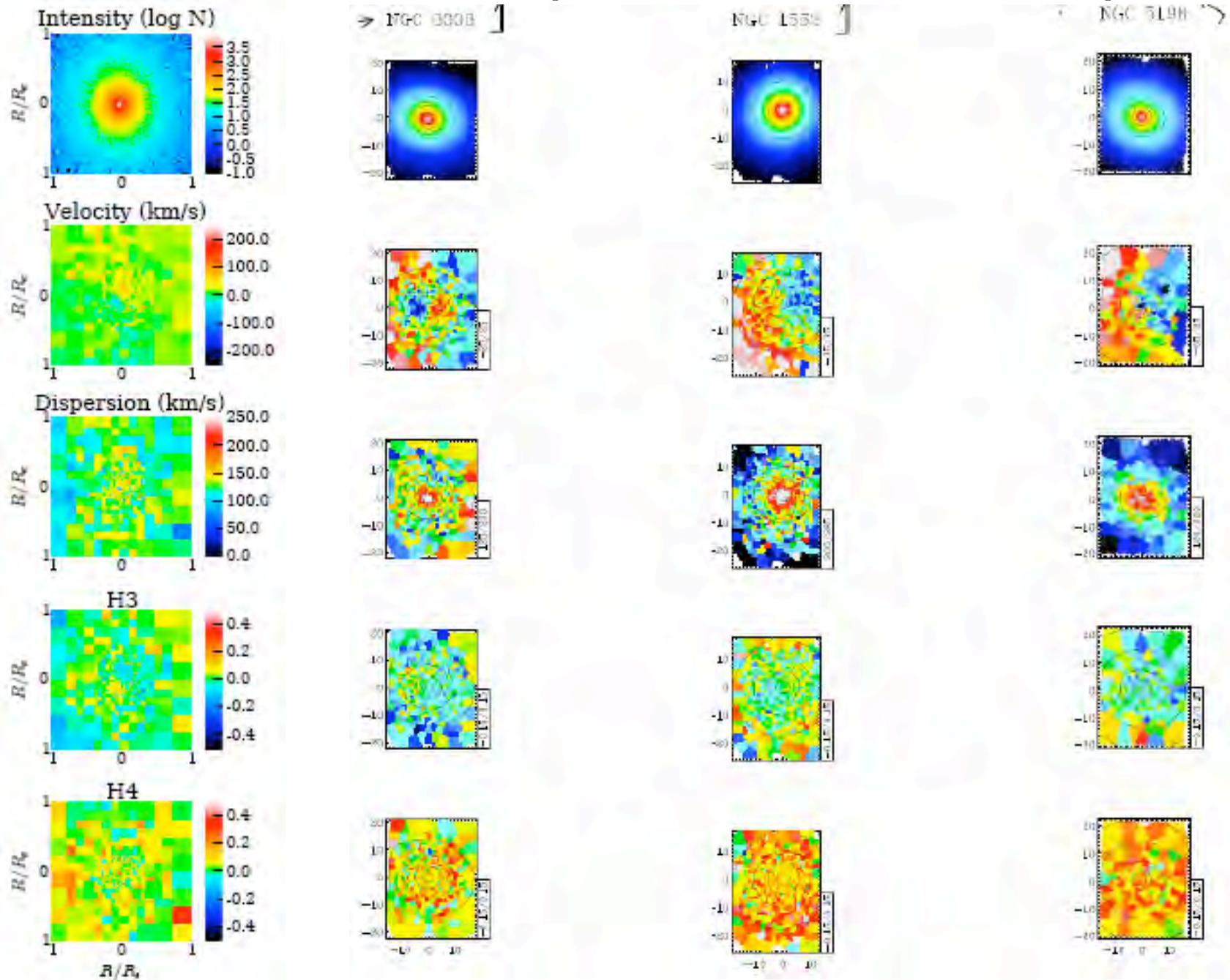
R_{eff} prediction by
 Cole et al. 2000
 dissipationless model

Covington et al. 2007 model
 also works well for non-equal
 mass mergers, including minor
 mergers!



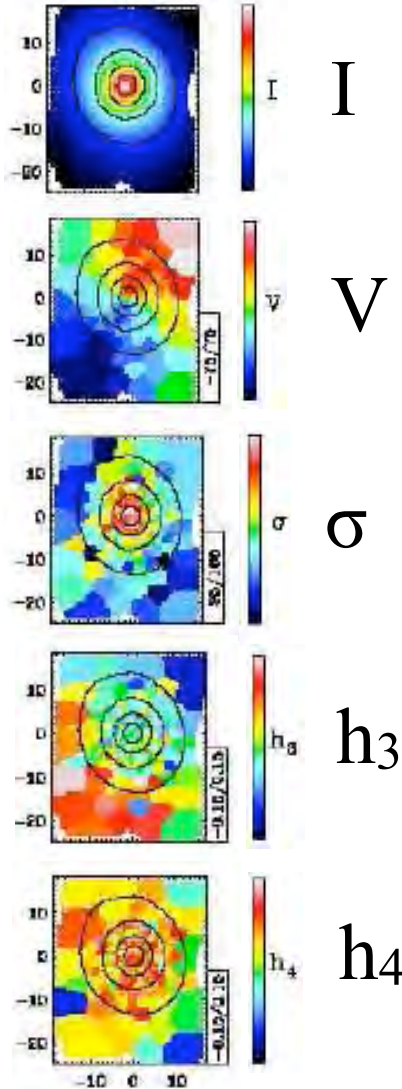
Stellar velocity
 dispersion also
 predicted well!

SAURON Data (from Emsellem et al. 2004)

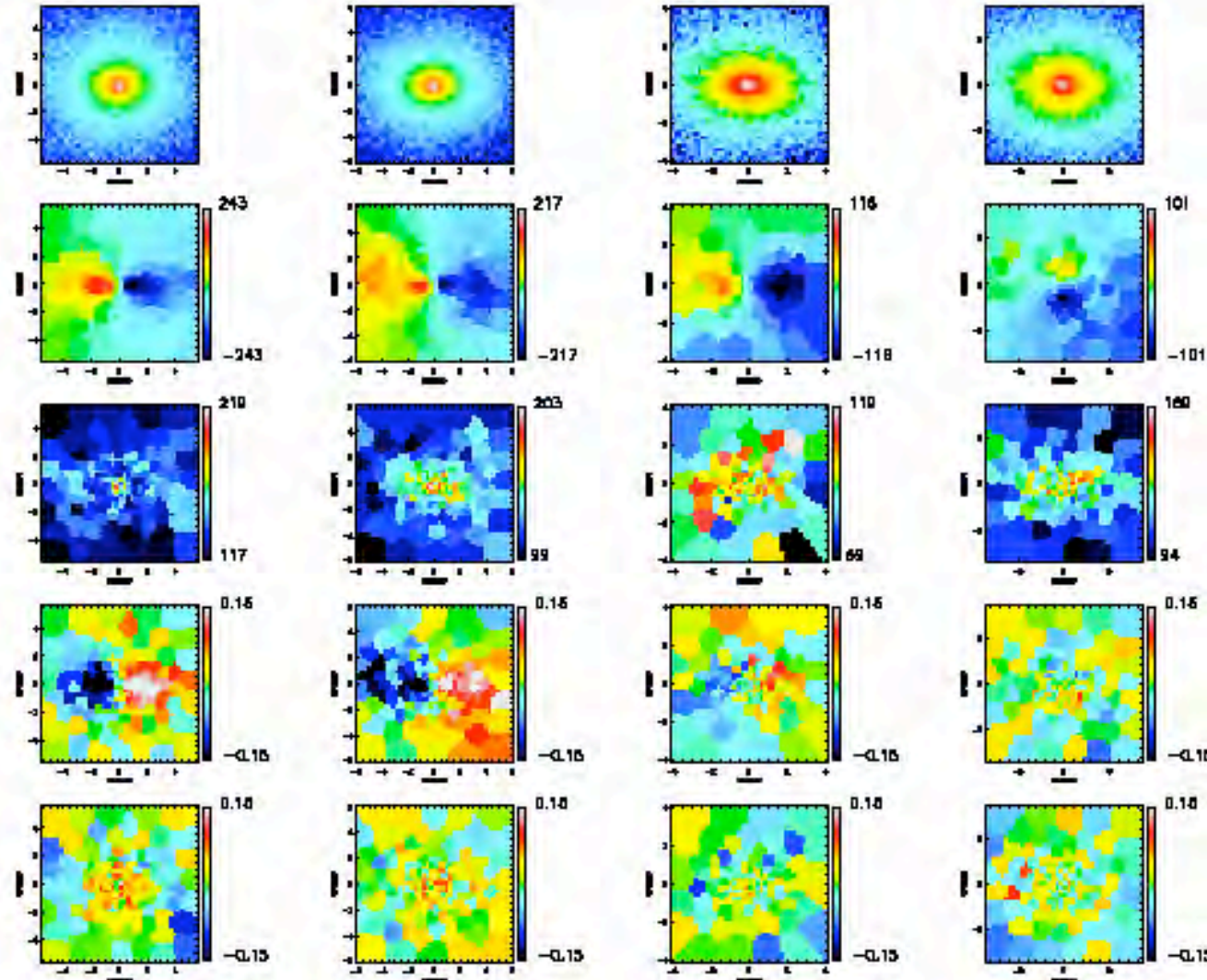


Comparison with SAURON data in progress by UCSC grad student Greg Novak working with Cox, Jonsson, Faber, and Primack.

NGC 474



Views of G3G3 merger, plotted like SAURON data.



The **conclusions** so far from the SAURON comparison are:

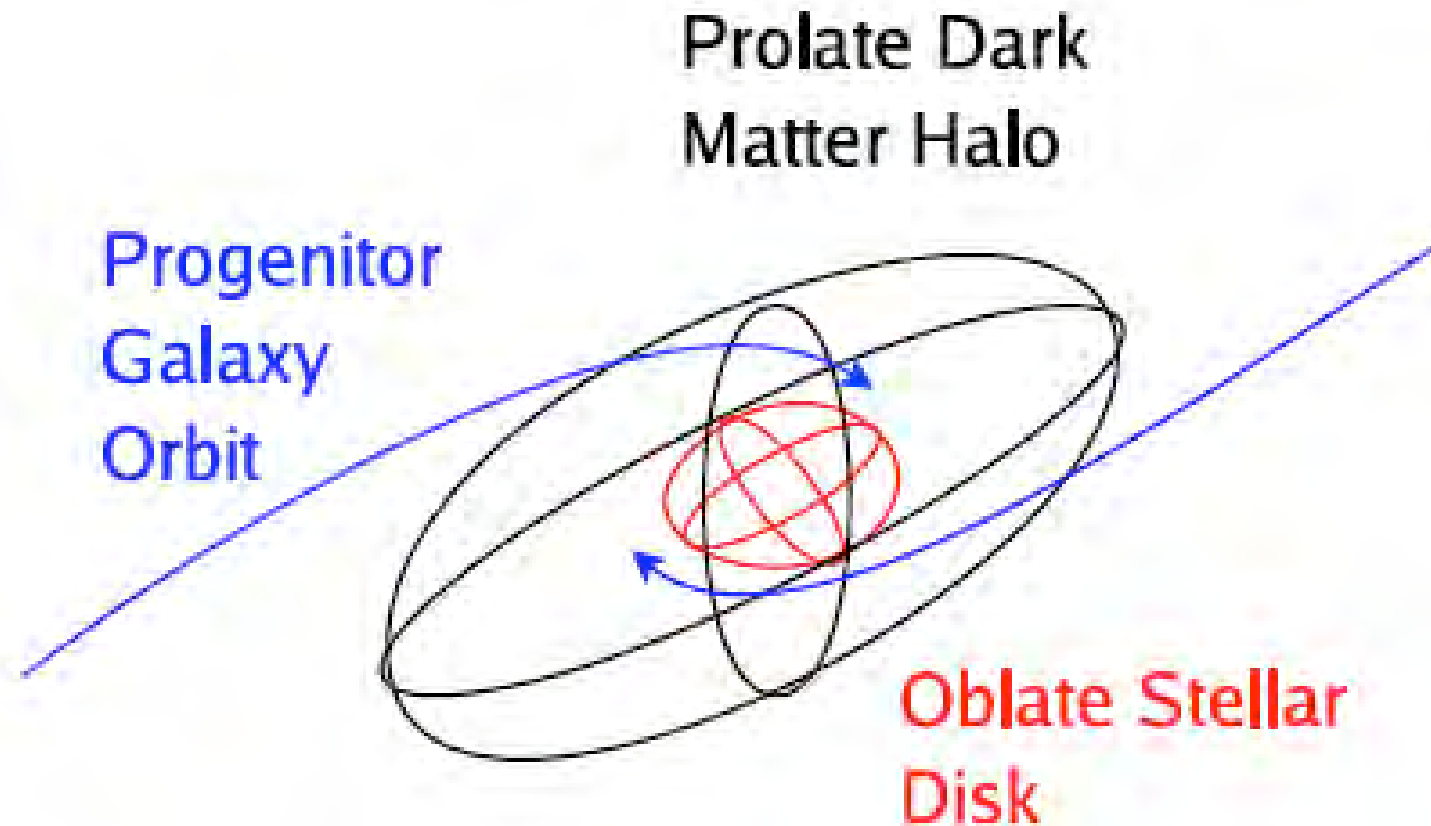
1) Binary hydrodynamic major mergers form qualitatively similar replicas of the SAURON "fast rotator" early type galaxies ($\sim 2/3$?).

2) Binary **gas-poor** major-mergers spiral galaxy and binary gas poor elliptical-elliptical mergers **cannot** form the SAURON "fast rotators." They have too little rotation and get the V-H3 correlation wrong.

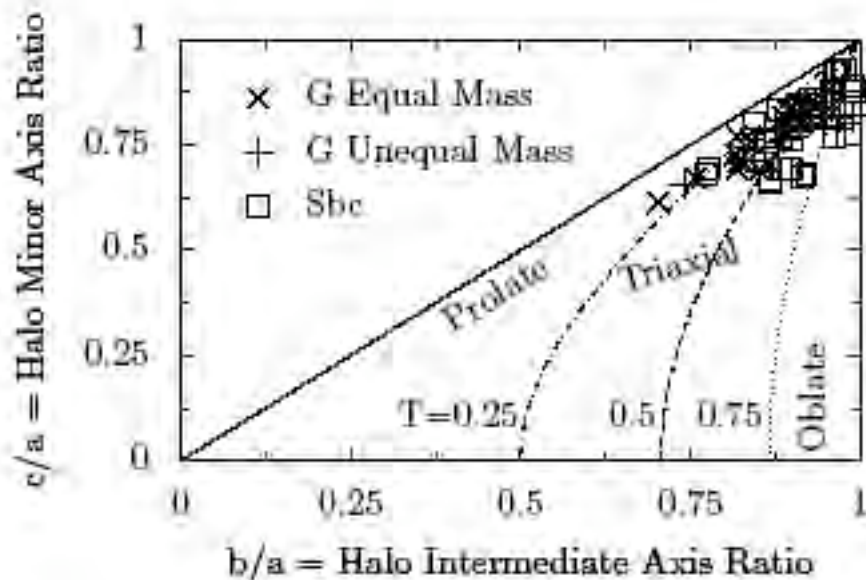
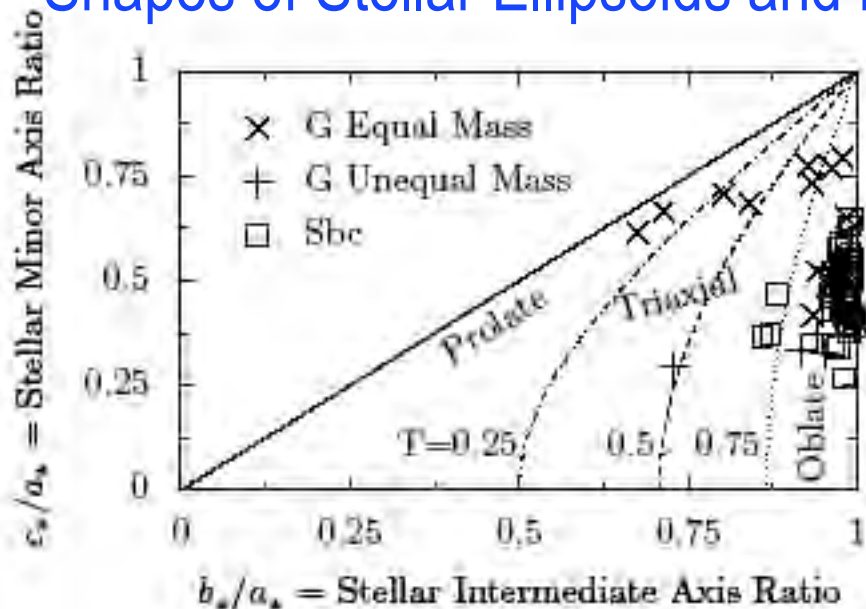
3) Binary **gas-poor** major-mergers spiral galaxy and binary gas poor elliptical-elliptical mergers **probably can't** form the SAURON slow rotators ($\sim 1/3$), **unless** slow rotators are significantly more elliptical on average than is indicated by the SAURON survey. Greg Novak is running various types of multiple hydrodynamic mergers to try to form galaxies like the SAURON slow rotators.

The short (rotation) axis of the visible elliptical galaxy is perpendicular to the long axis of its dark matter halo.

Why? The long axis of the halo is along the merger axis, while the angular momentum axis is perpendicular to that axis.



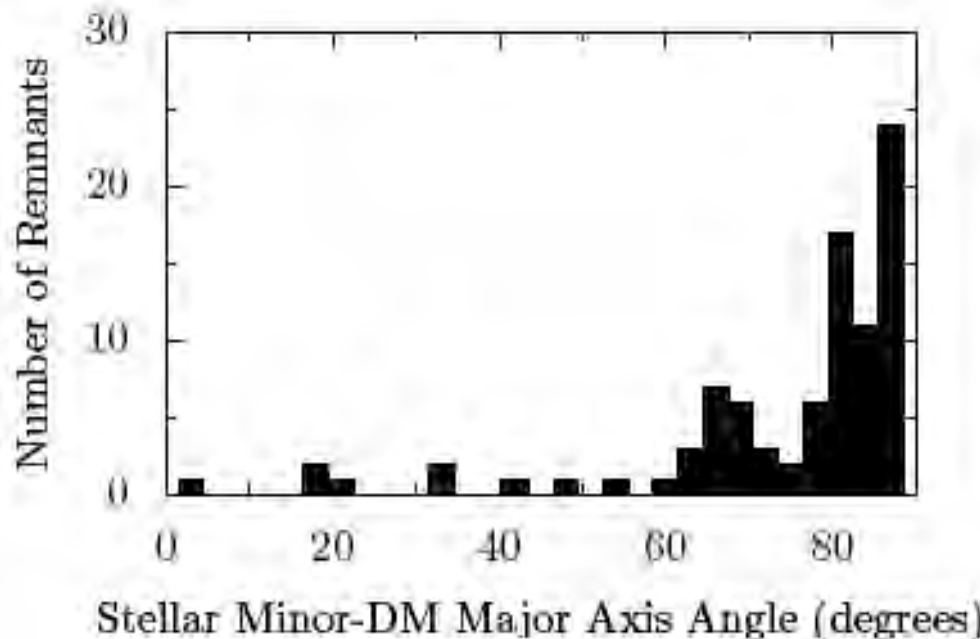
Shapes of Stellar Ellipsoids and Dark Halos of Major Merger Remnants



The stellar ellipsoids are mostly oblate but the dark matter halo is usually triaxial or prolate.

The stellar minor axis usually aligns with the angular momentum axis, which aligns with the dark matter smallest axis, perpendicular to the dark matter major axis.

Novak, Cox, Primack, Jonsson, & Dekel, ApJ Letters 2006



Simulations of Dust in Interacting Galaxies

**Patrik
Jonsson**

UCSC



HST image of “The Antennae”

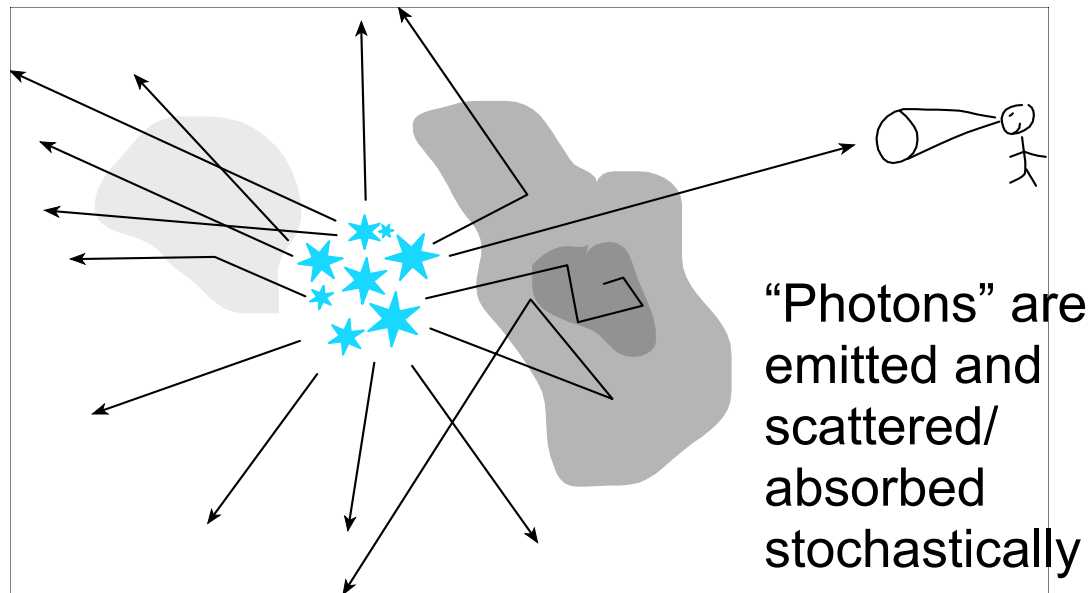
Introduction

- **Dust in galaxies is important**
 - Absorbs about 40% of the local bolometric luminosity
 - Makes brightness of spirals inclination-dependent
 - Completely hides the most spectacular bursts of star formation
 - Makes high-redshift SF history very uncertain
- **Dust in galaxies is complicated**
 - The mixed geometry of stars and dust makes dust effects geometry-dependent and nontrivial to deduce
 - Needs full radiative transfer model to calculate realistically
- **Previous efforts have used 2 strategies**
 - Assume a simple, schematic geometry like exponential disks, or
 - Simulate star-forming regions in some detail, assuming the galaxy is made up of such independent regions
 - Have not used information from N-body simulations

Our Approach

For every simulation snapshot:

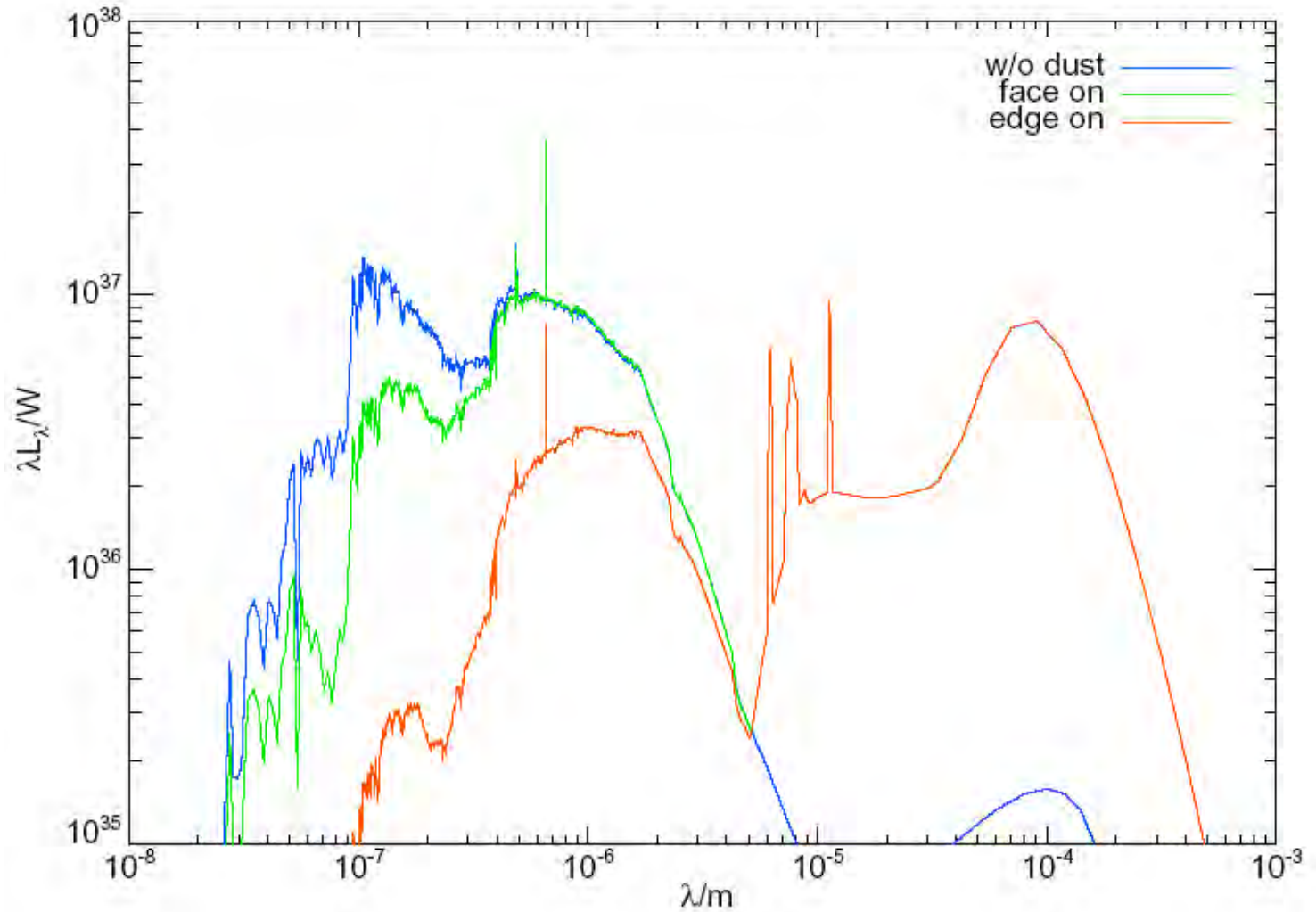
- SED calculation
- Adaptive grid construction
- Monte Carlo radiative transfer



Sunrise Radiative Transfer Code

- Run entire SED at once without scattering -- determines unabsorbed SED
- Run with scattering for a single wavelength; repeat for all wavelengths desired - code includes Ly alpha, beta; interpolate SED to full resolution
- New “polychromatic” method does wide range of wavelengths simultaneously, saves factor of ~100 computer time!
- Now incorporating “Mappings” to model HII regions in starbursts

Spectral Energy Distribution



Monochromatic vs. Polychromatic Radiative Transfer Models

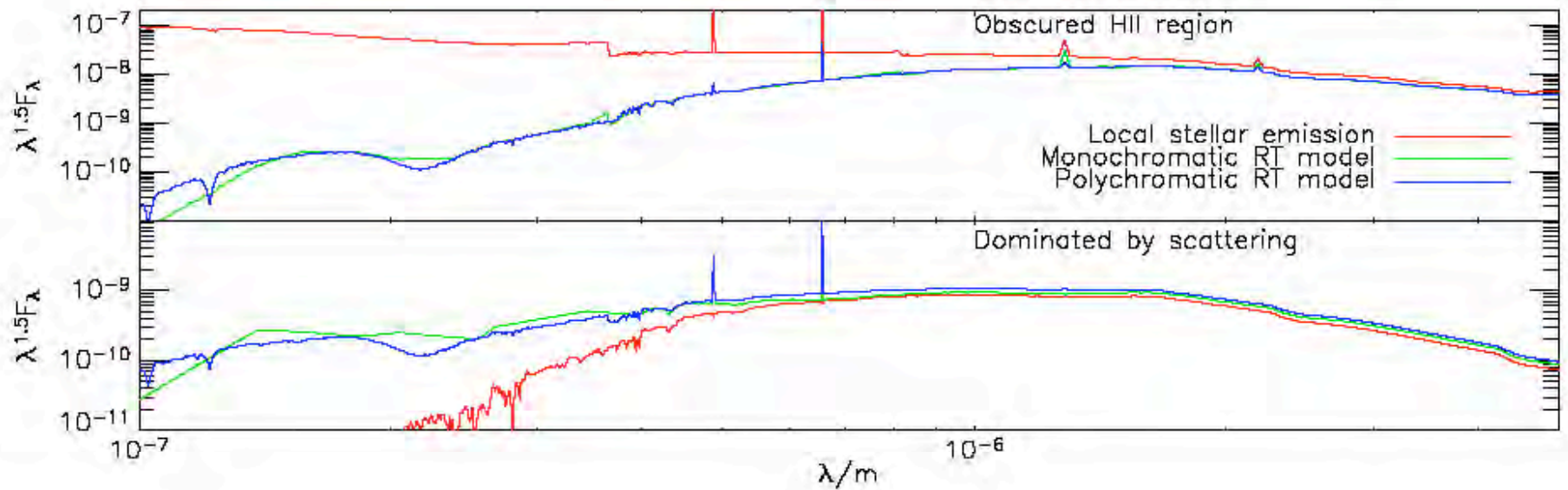
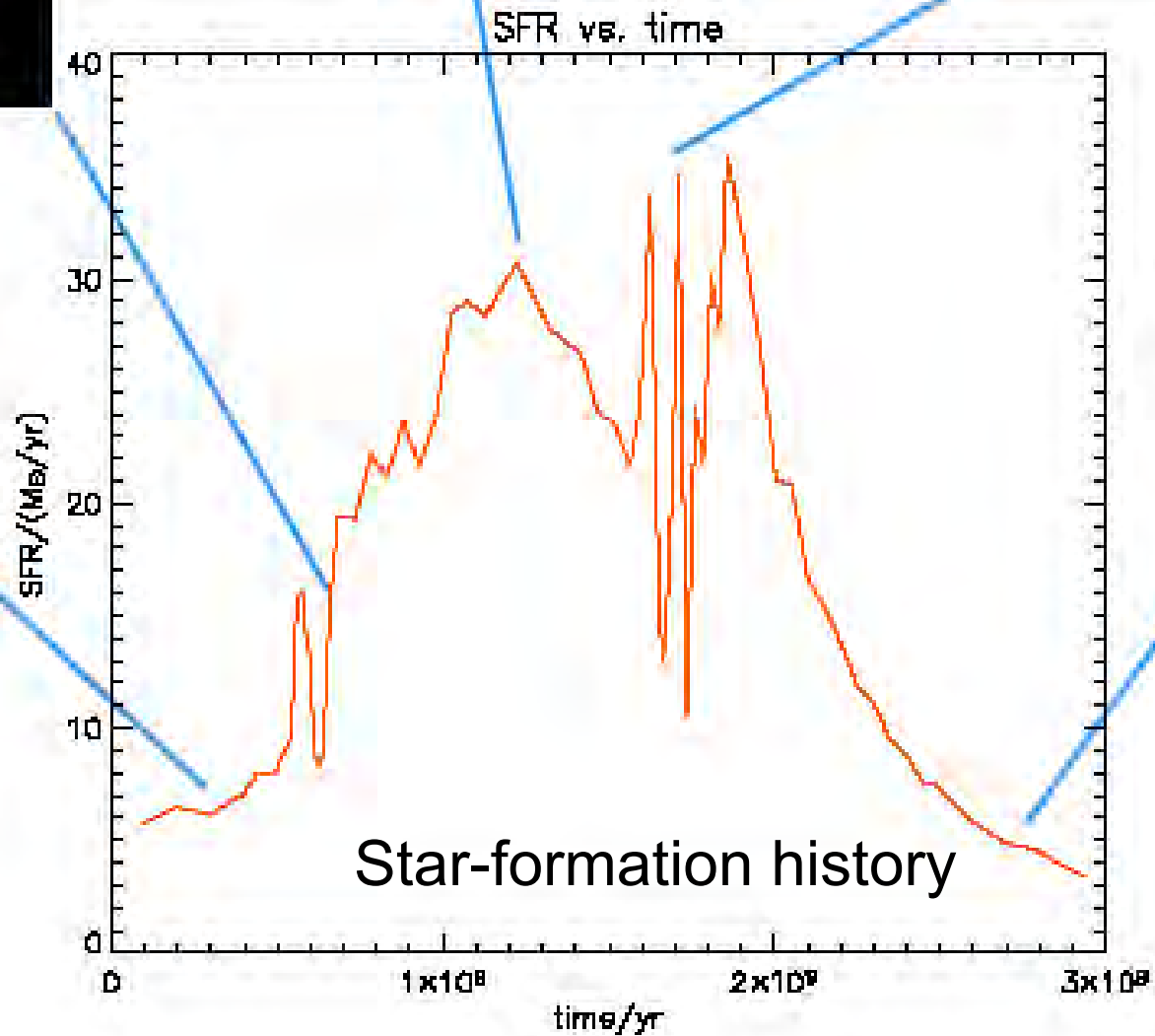
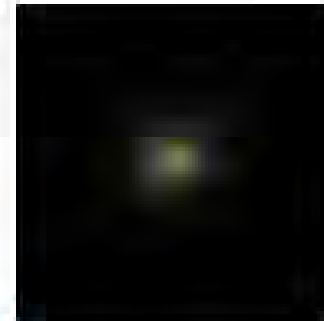
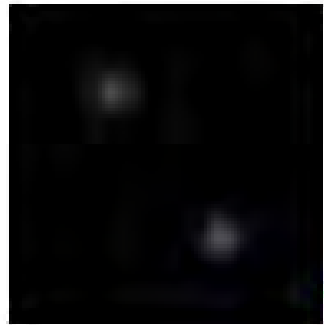
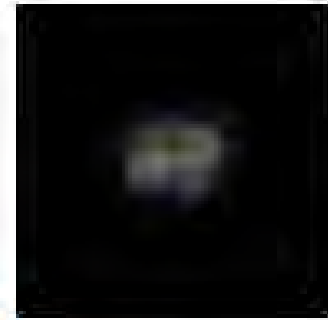
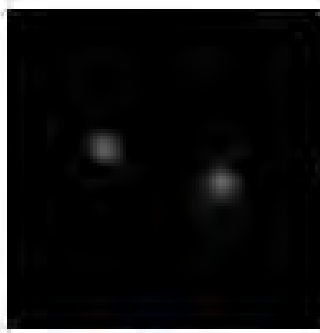
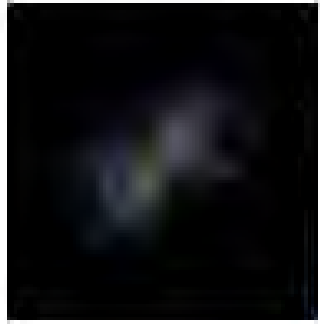
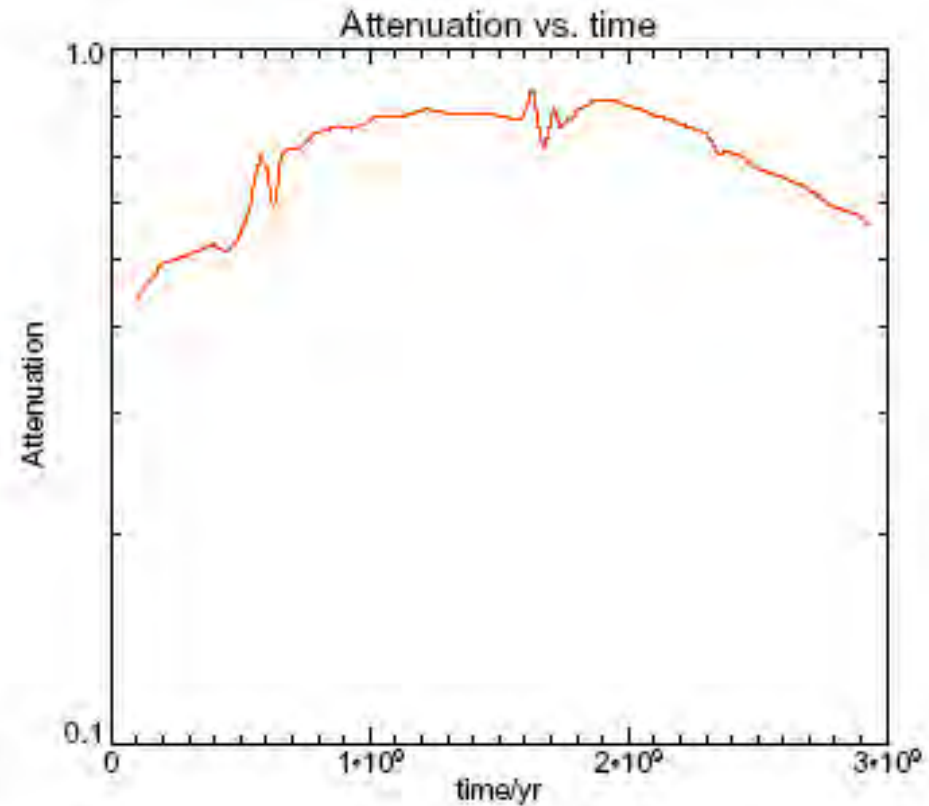
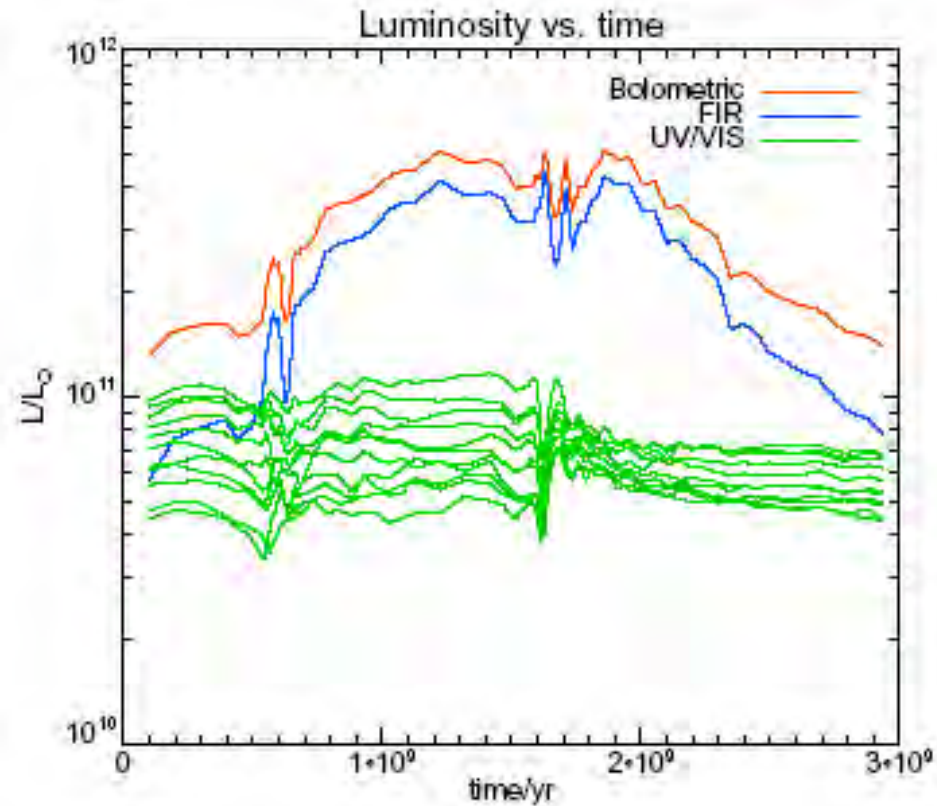


Figure 8. Spectra from the galaxy merger simulations, exemplifying the effects of the new polychromatic algorithm. In both images, the red line shows the intrinsic emission in the pixel, neglecting radiative-transfer effects. The green line shows the old algorithm, where the spectrum is interpolated between 20 discrete wavelengths, and the blue line is the result from the polychromatic radiative transfer. The top plot shows a pixel containing an obscured HII region, the bottom plot a pixel near an HII region where the UV flux is dominated by scattered light. While the results agree well on the overall spectral shape, the new method gives significantly more realistic results especially for the small-scale spectral features, at a fraction of the runtime. Note in particular how the polychromatic algorithm predicts the appearance of the Ly α absorption line, the disappearance of the nebular Balmer continuum edge, and the increased attenuation of the Paschen β line at $1.3 \mu\text{m}$ in the spectrum of the HII region. The polychromatic calculation, including 500 wavelengths, used about 8 times the CPU time required for one monochromatic calculation. With monochromatic ray tracing, 500 separate wavelengths would have to be used to predict the same amount of detail, which would require a factor of 50 more CPU time.

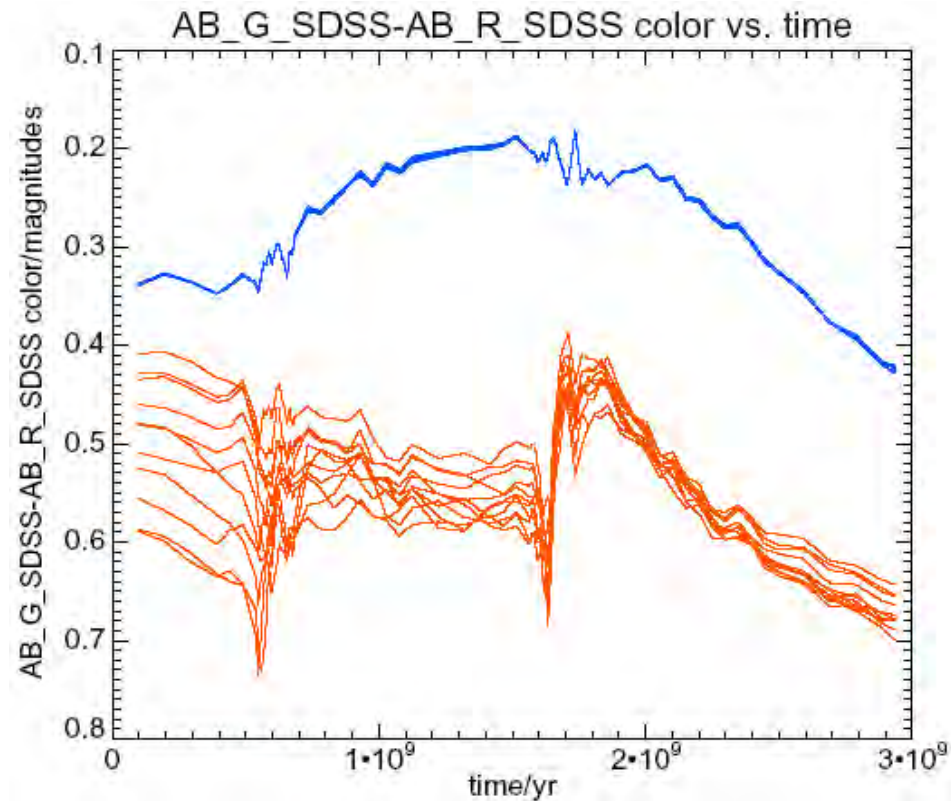
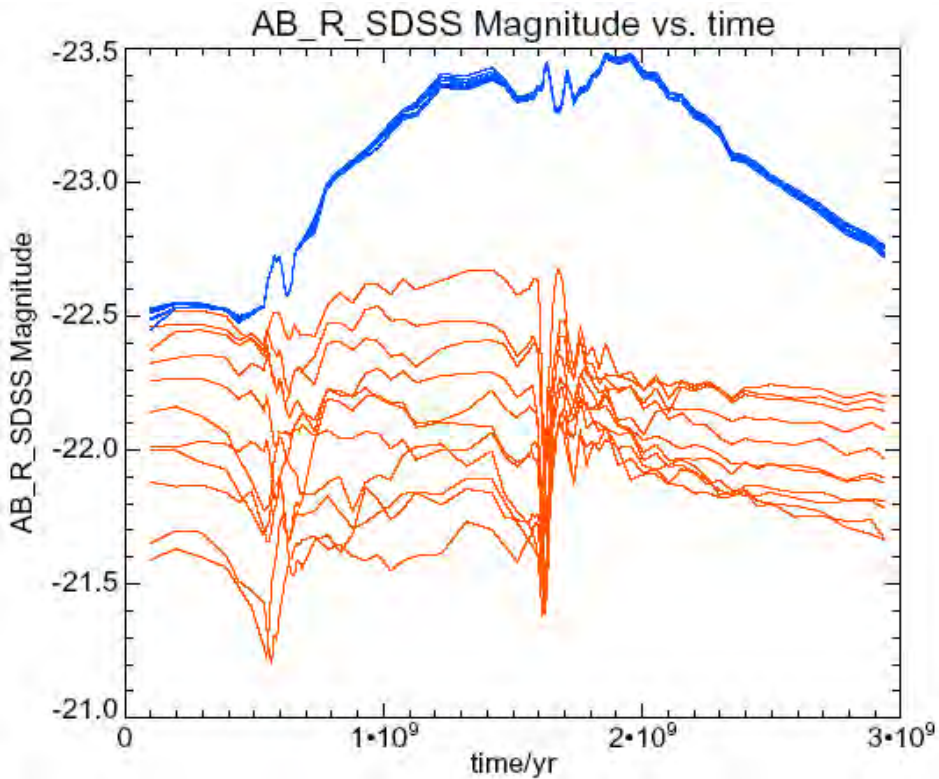


Luminosities



UV/visual luminosity is practically constant over time
Attenuation increases with bolometric luminosity

Magnitudes & Colors

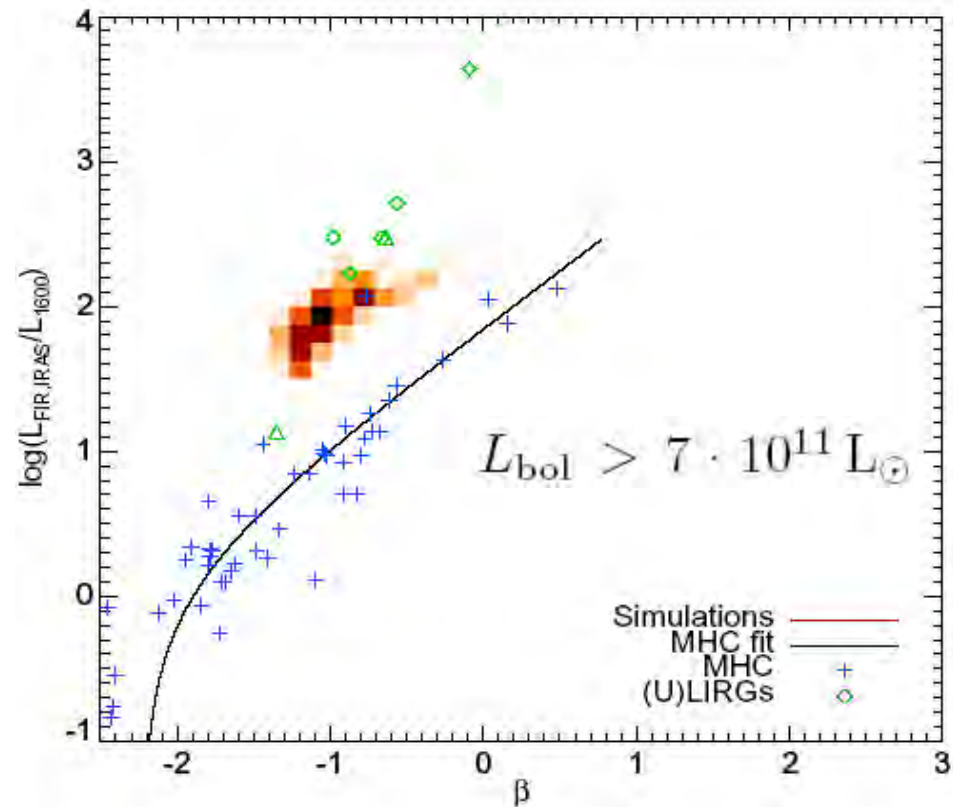
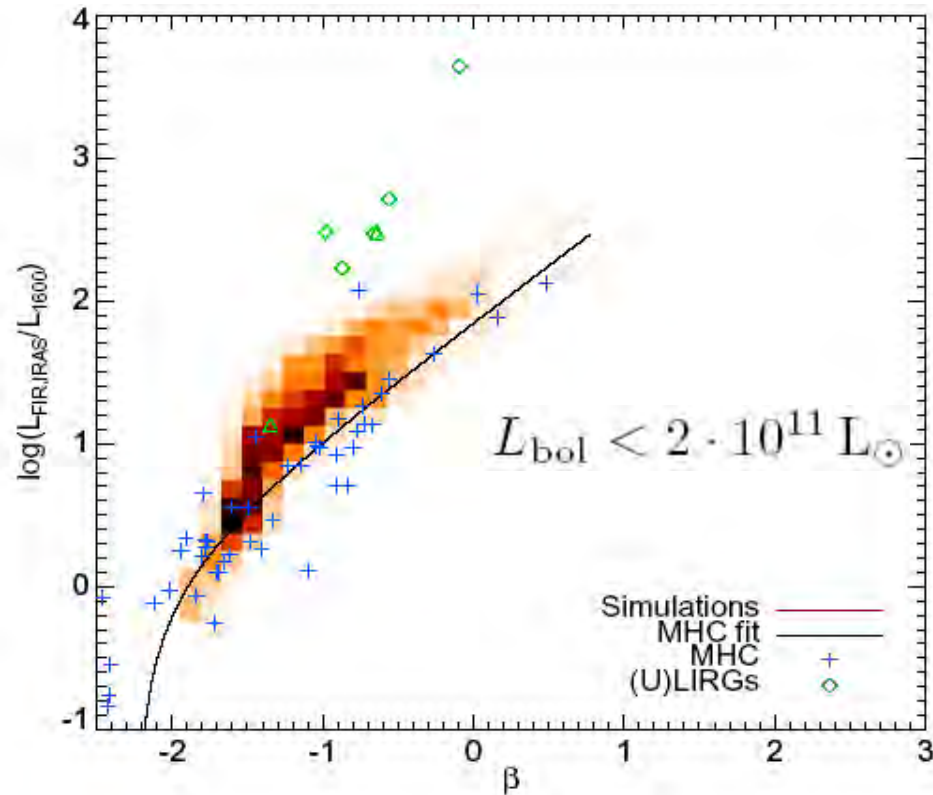


During the transients, the magnitudes and colors with and without dust are **anticorrelated**

Comparing to IRX-Beta relation

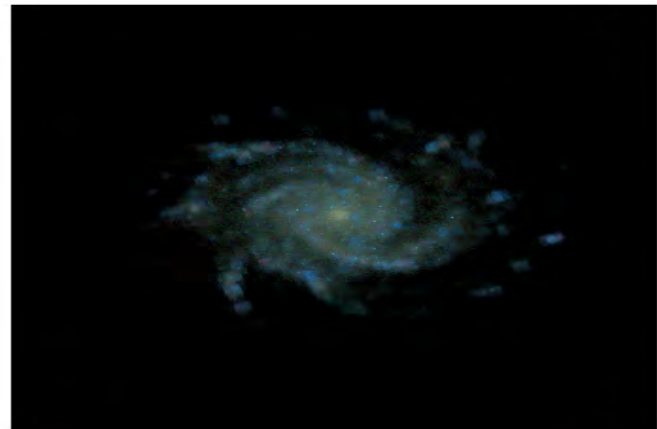
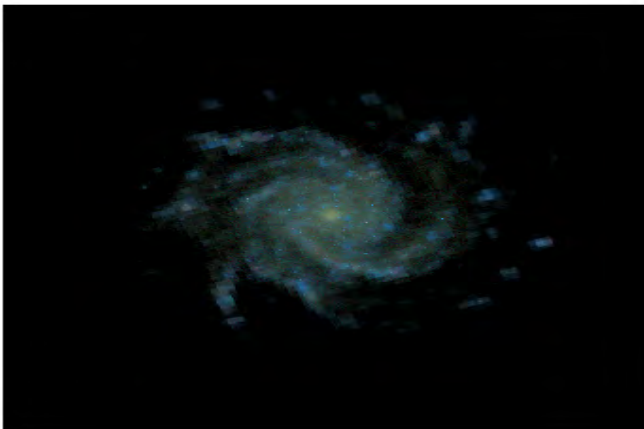
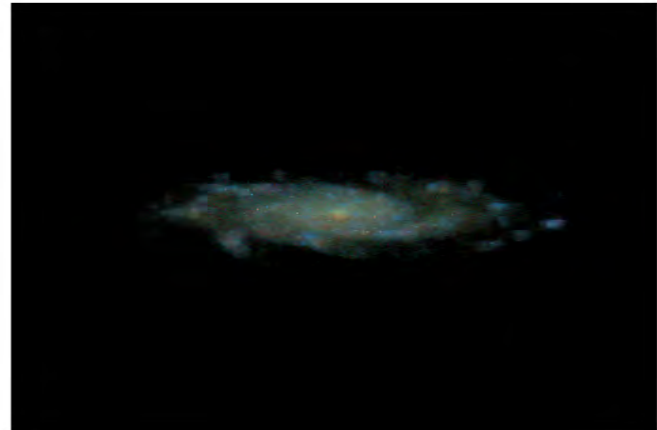
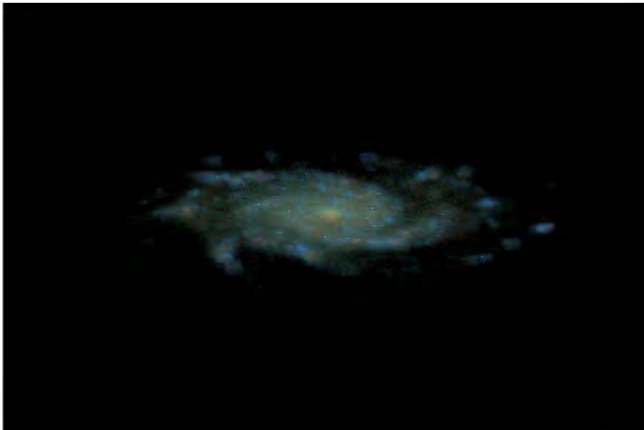
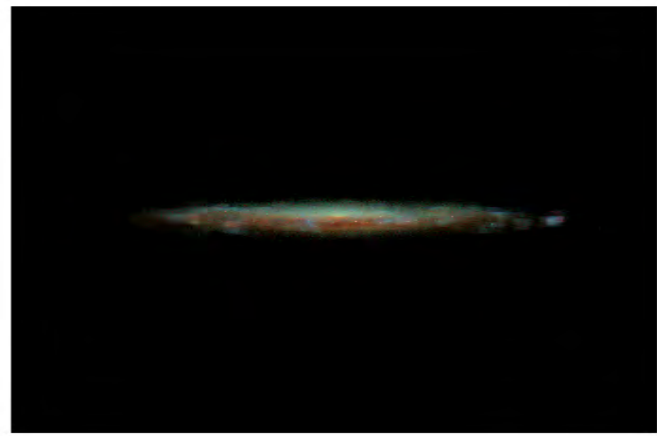
- $IRX_{1600} = F_{FIR}/F_{1600}$,
- UV spectral slope β_U
Determined by fitting $f_\lambda \propto \lambda^\beta$.
- Observed sample is starbursts observed with IUE (Meurer, Heckman, Calzetti 99)
- Also ULIRGS (Goldader 02)

Split by Luminosity

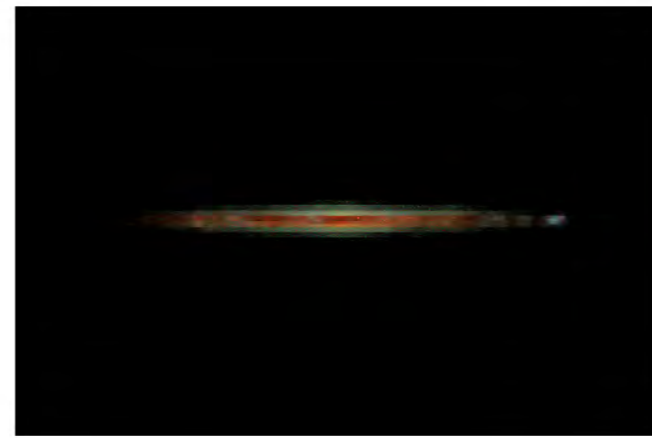
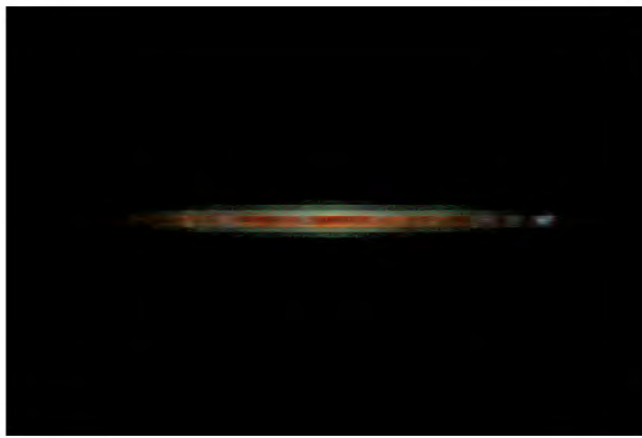


- Simulated lower-luminosity galaxies follow an IRX- β relation similar to the observed MHC99 galaxies
- Higher-luminosity galaxies occupy the UIRG region
- Note that these were predictions: no parameter fitting!

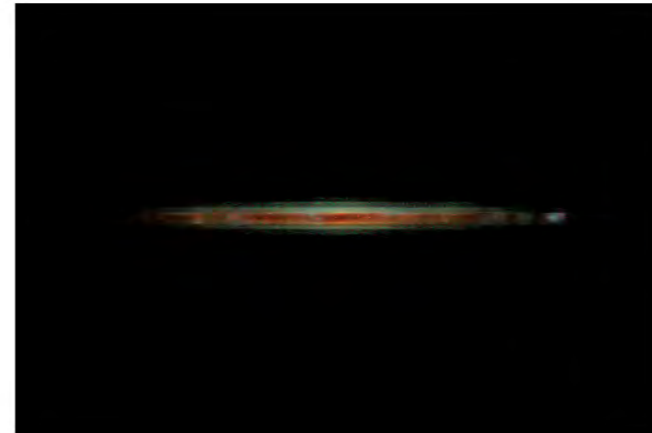
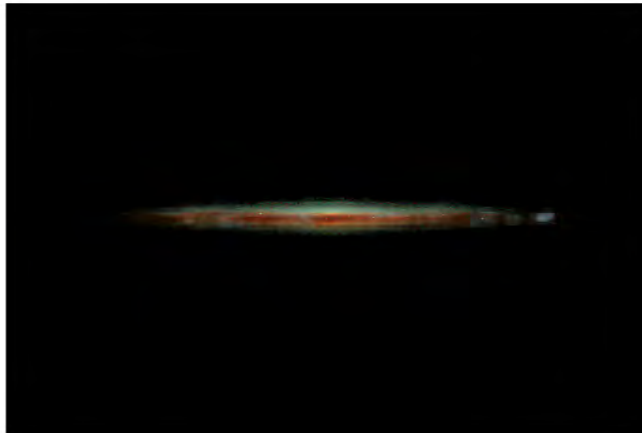
Images of
quiescent disk
galaxies with
effects of dust
from *Sunrise*
Monte Carlo
radiative transfer
code



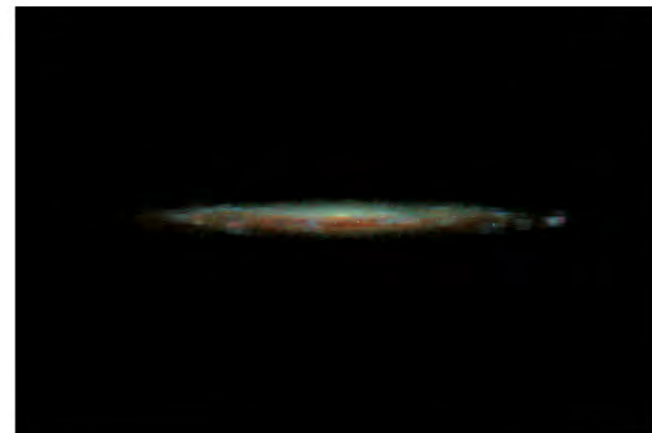
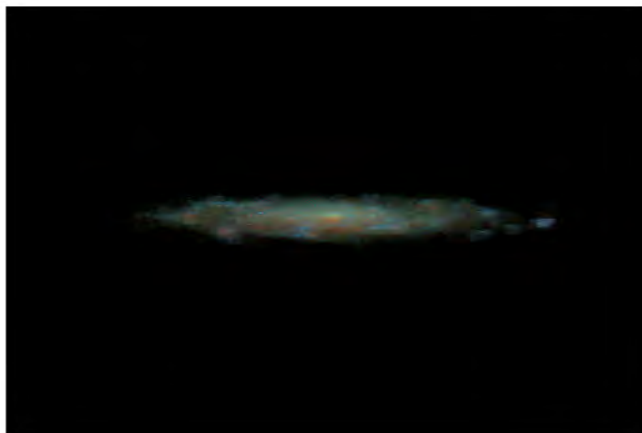
Near edge-on
images (with dust)
from *Sunrise* Monte
Carlo radiative
transfer code



These were run
with no radial
metallicity gradient,
but our latest work
shows that
observed radial
gradients predict
attenuation vs.



inclination in
agreement with
observations --
[Miguel Rocha,
Jonsson, JP, & Cox
2006 MN in press](#)



Dust Attenuation in Hydrodynamic
Simulations of Spiral Galaxies
Rocha, Jonsson, Primack, & Cox 2007 MN

Right hand side:
Xilouris et al. 1999
metallicity gradient

Sbc - no dust



Sbc - Xilouris
metallicity gradient



Sbc - constant
metallicity gradient



50 Kpc

50 Kpc

Sbc



G3



G2

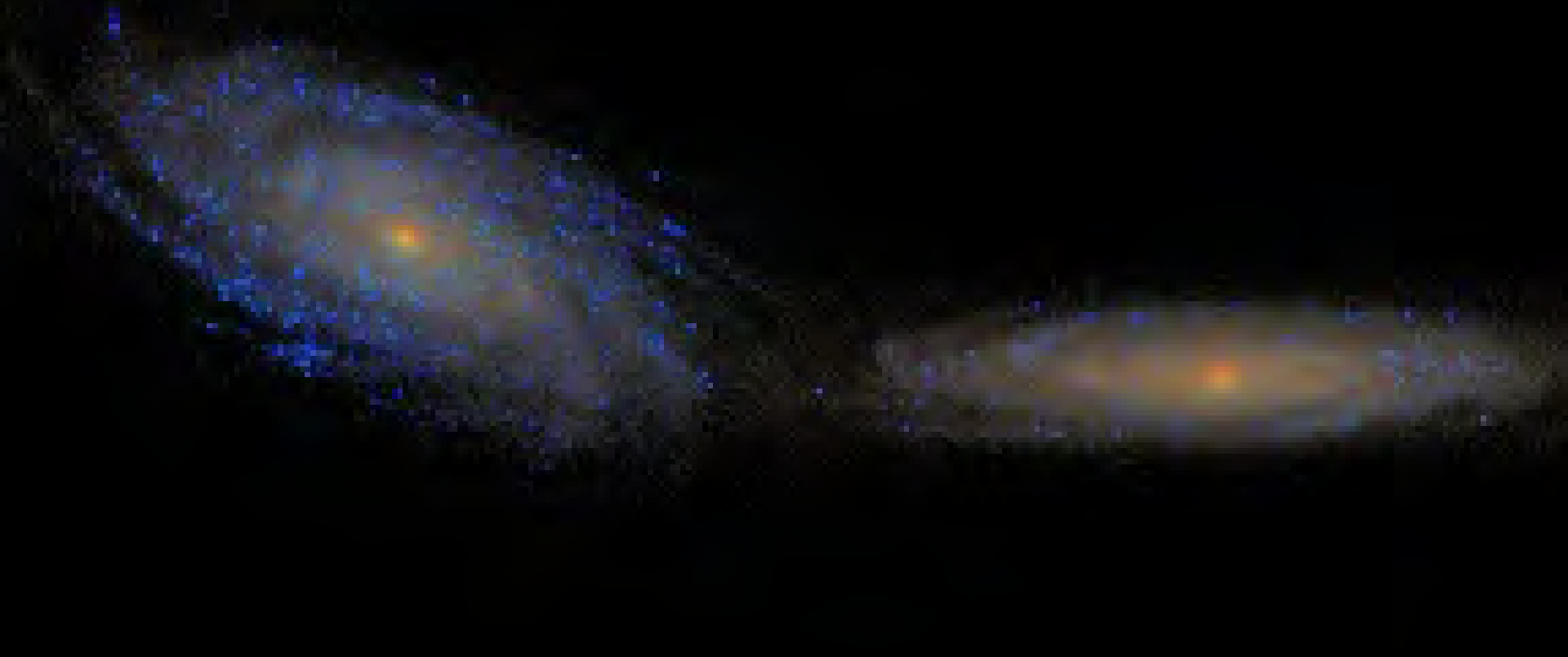


G1



Galaxy Merger Simulation

run on the Columbia Supercomputer
by Greg Novak and Patrik Jonsson



This and the following images show a merger between two Sbc galaxies, each simulated with 1.7 million particles (10x more than the previous images), and with dust absorption computed with $\sim 10^6$ rays per image. The images are realistic color composites of u, r, and z-band images.





Galaxy Merger Simulation

run on the Columbia Supercomputer
(music by Nancy Abrams)



Predictions from Galaxy
Modeling:

Quantifying Galaxy
Morphology and
Identifying Mergers

see Lotz, Primack & Madau 2004, AJ, 128,
163; ApJ in press; and papers in final prep.

ULIRGS Borne et al. (2000)

Measuring Galaxy Morphology

- by “eye” - Hubble tuning fork E-Sa-Sb-Sc-Sd-(Irr)
 - parametric
 - 1-D profile fit ($r^{1/4}$, exponential, Sersic)
 - 2-D profile fit (bulge+disk; GIM2D, GALFIT)
 - doesn't work for irregular/merging galaxies
 - non-parametric
 - “CAS” - concentration, asymmetry, clumpiness
 - neural-net training
 - shaplet decomposition
- new: Gini Coefficient (Abraham et al. 2003)**
M₂₀ 2nd order moment of brightest regions

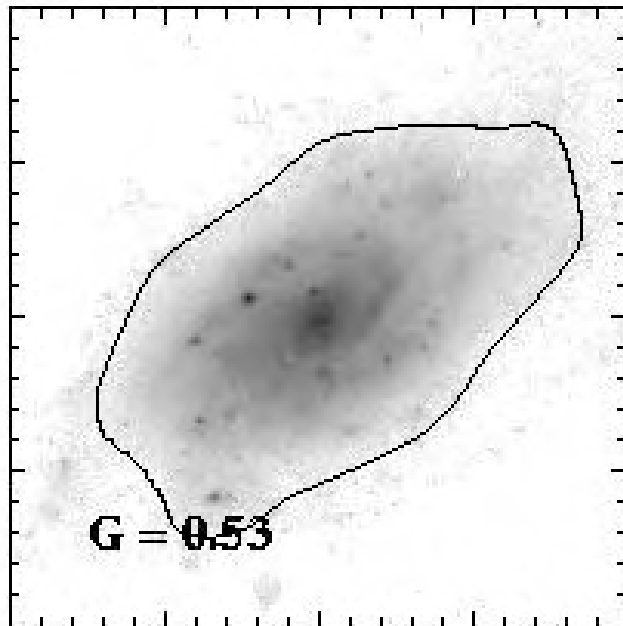
The Gini Coefficient

used in economics to measure distribution of wealth in population
→ distribution of flux in galaxy's pixels (Abraham et al. 2003)

$G=0$ for completely egalitarian society (uniform surf brightness)

$G=1$ for absolute monarchy (all flux in single pixel)

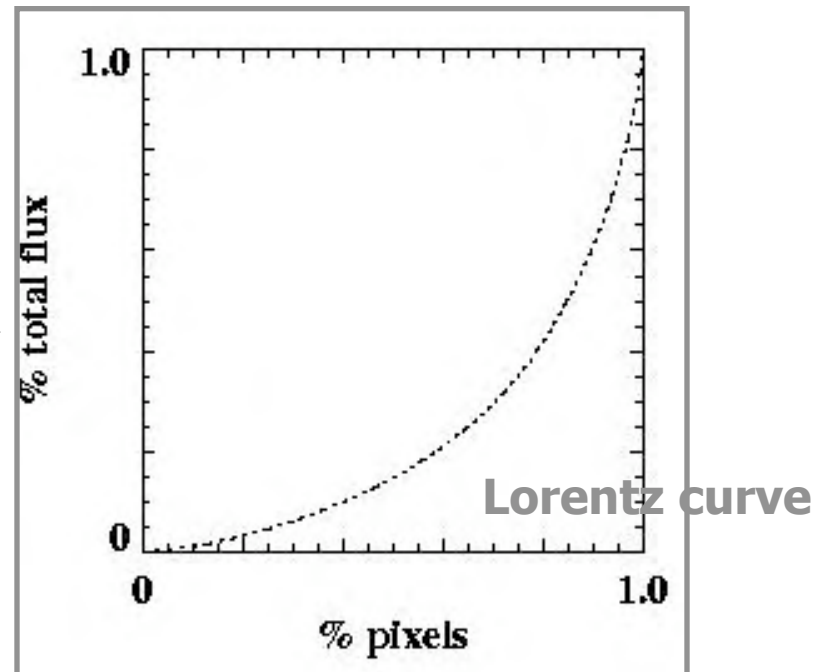
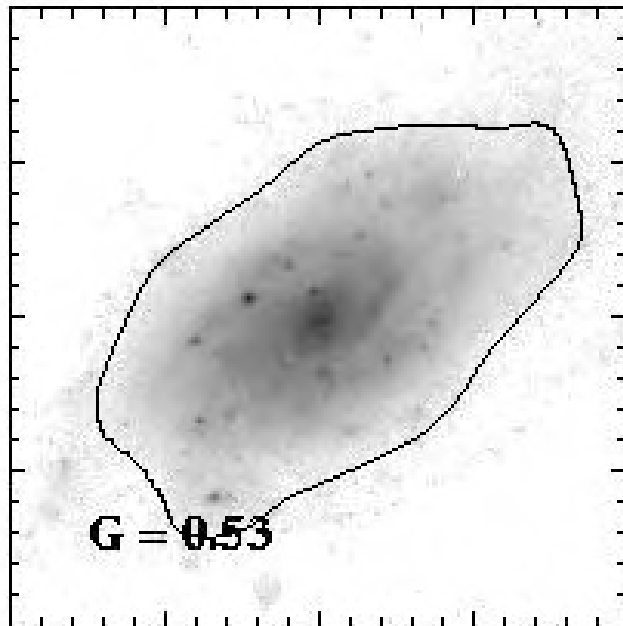
($G = 0.445$ for US in 1999)



The Gini Coefficient

used in economics to measure distribution of wealth in population
→ distribution of flux in galaxy's pixels (Abraham et al. 2003)

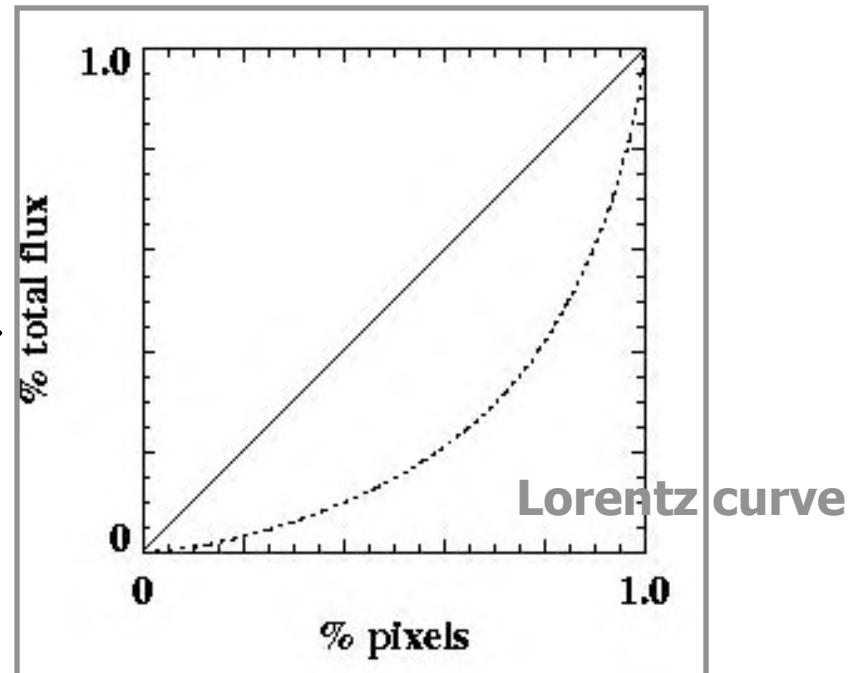
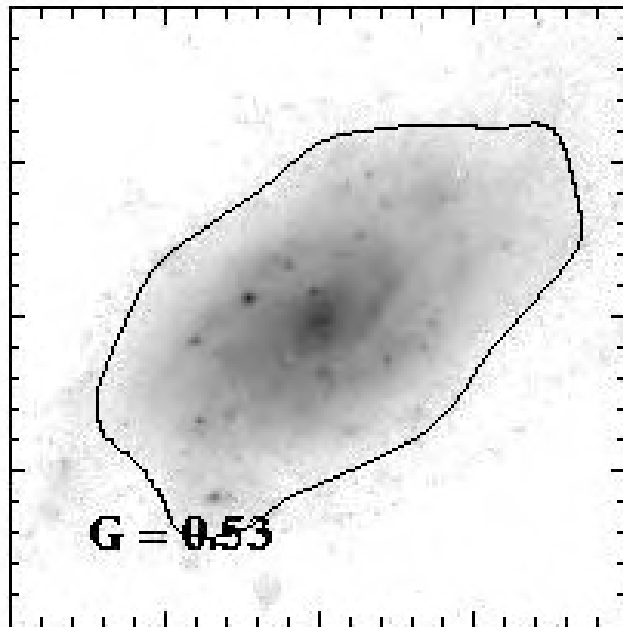
$G=0$ for completely egalitarian society (uniform surf brightness)
 $G=1$ for absolute monarchy (all flux in single pixel)
($G = 0.445$ for US in 1999)



The Gini Coefficient

used in economics to measure distribution of wealth in population
→ distribution of flux in galaxy's pixels (Abraham et al. 2003)

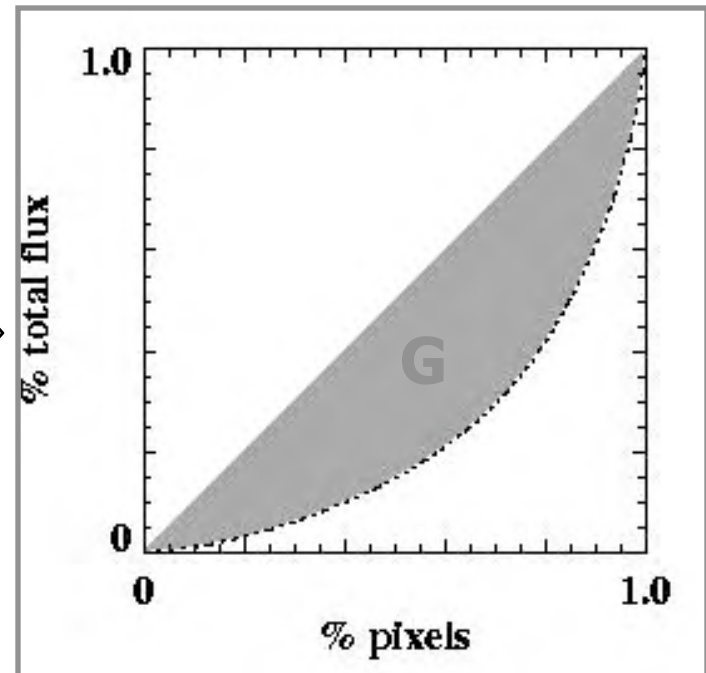
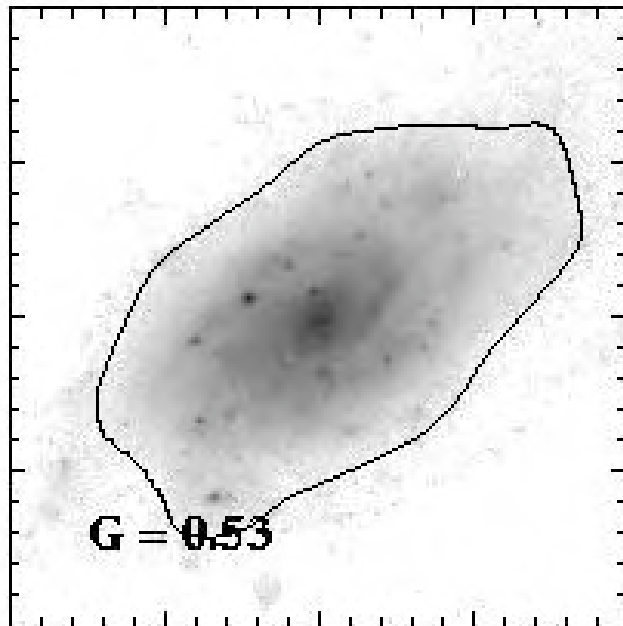
$G=0$ for completely egalitarian society (uniform surf brightness)
 $G=1$ for absolute monarchy (all flux in single pixel)
($G = 0.445$ for US in 1999)



The Gini Coefficient

used in economics to measure distribution of wealth in population
→ distribution of flux in galaxy's pixels (Abraham et al. 2003)

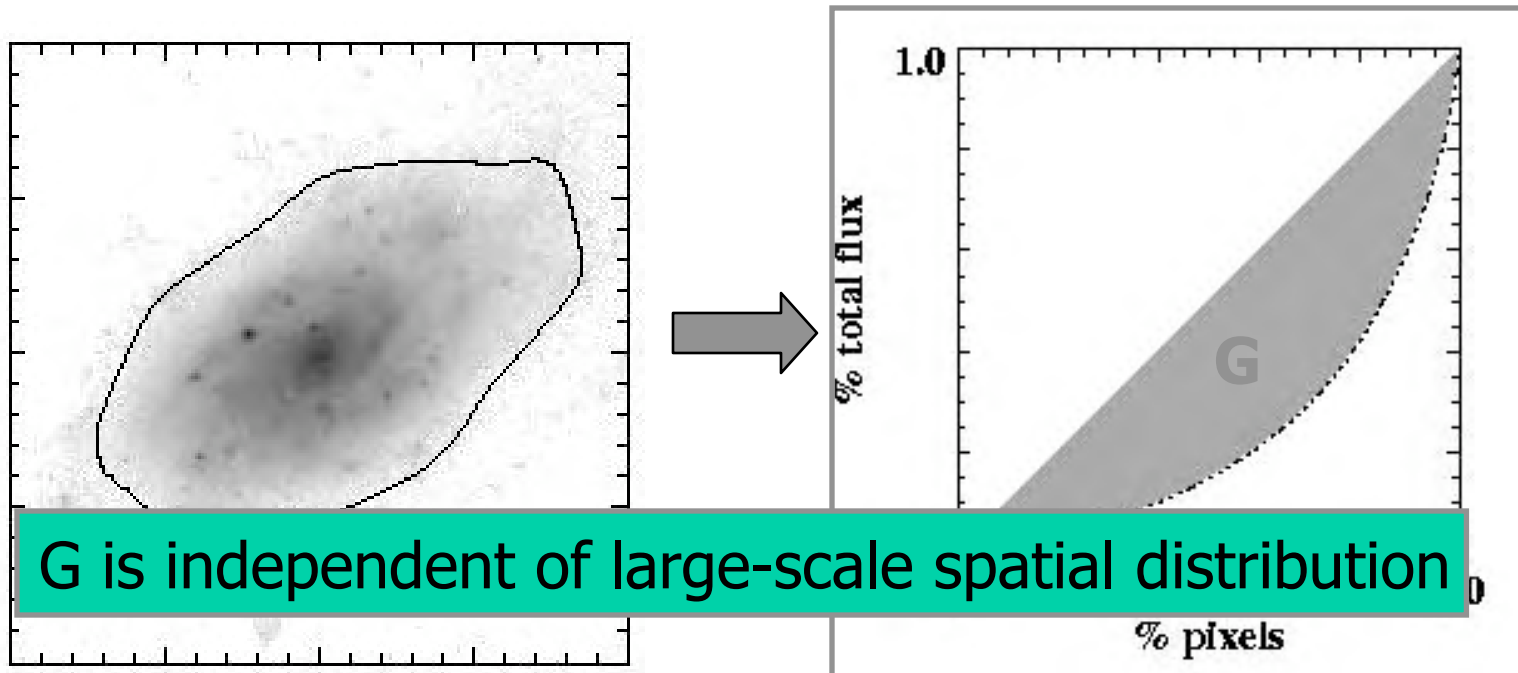
$G=0$ for completely egalitarian society (uniform surf brightness)
 $G=1$ for absolute monarchy (all flux in single pixel)
($G = 0.445$ for US in 1999)



The Gini Coefficient

used in economics to measure distribution of wealth in population
→ distribution of flux in galaxy's pixels (Abraham et al. 2003)

$G=0$ for completely egalitarian society (uniform surf brightness)
 $G=1$ for absolute monarchy (all flux in single pixel)
($G = 0.445$ for US in 1999)



2nd order moment of light

$$M_{\text{total}} = \sum f_i r_i^2 \quad (\text{minimize to find center of light})$$

this depends on size + luminosity

→ find relative moment of brightest regions

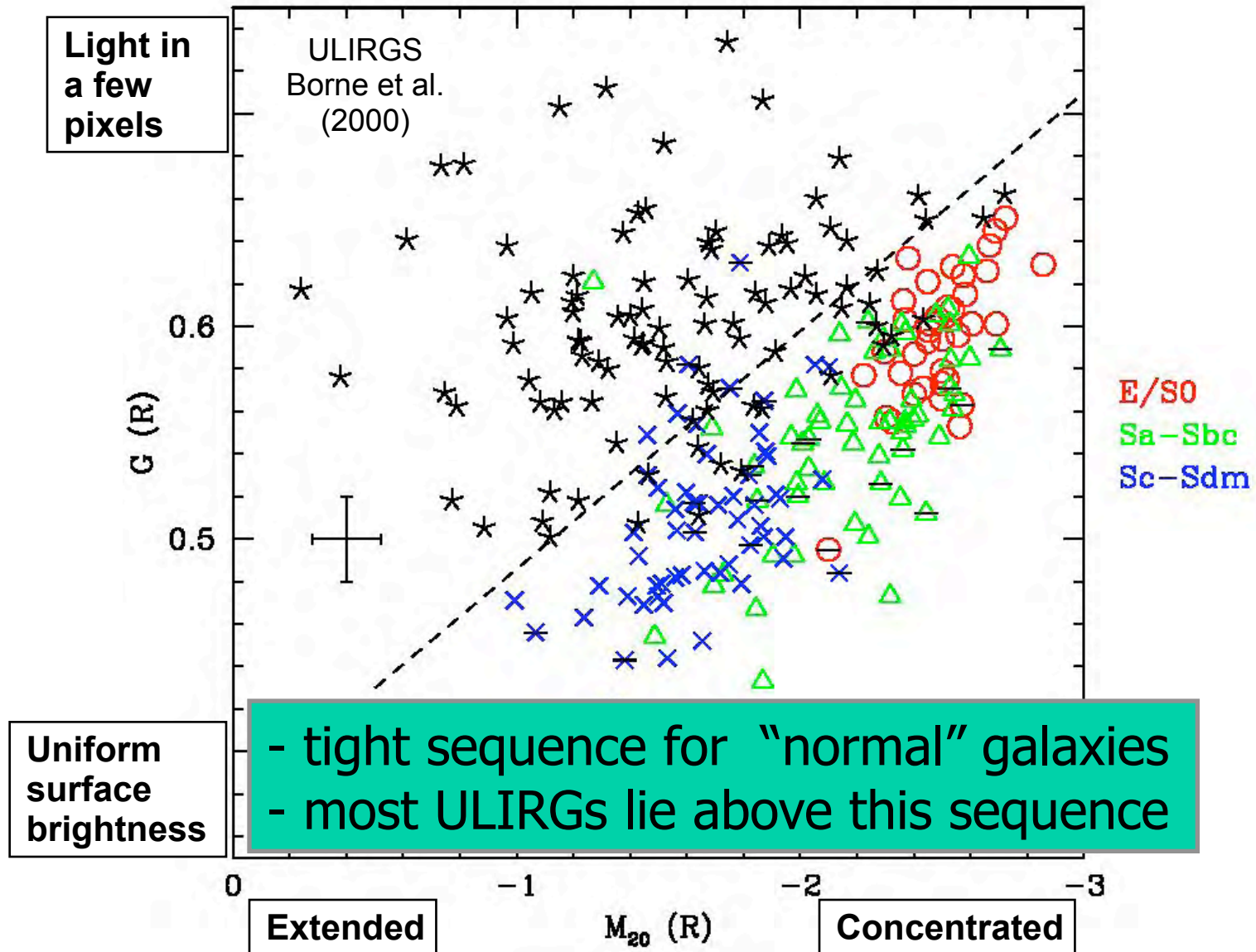
$$M_{20} = \log_{10} \frac{\sum_1^n f_i r_i^2}{M_{\text{total}}} \quad \text{where} \quad \sum_1^n f_i = 0.2 \sum f_i$$

- very similar to $C = \log (r_{80\%}/r_{20\%})$

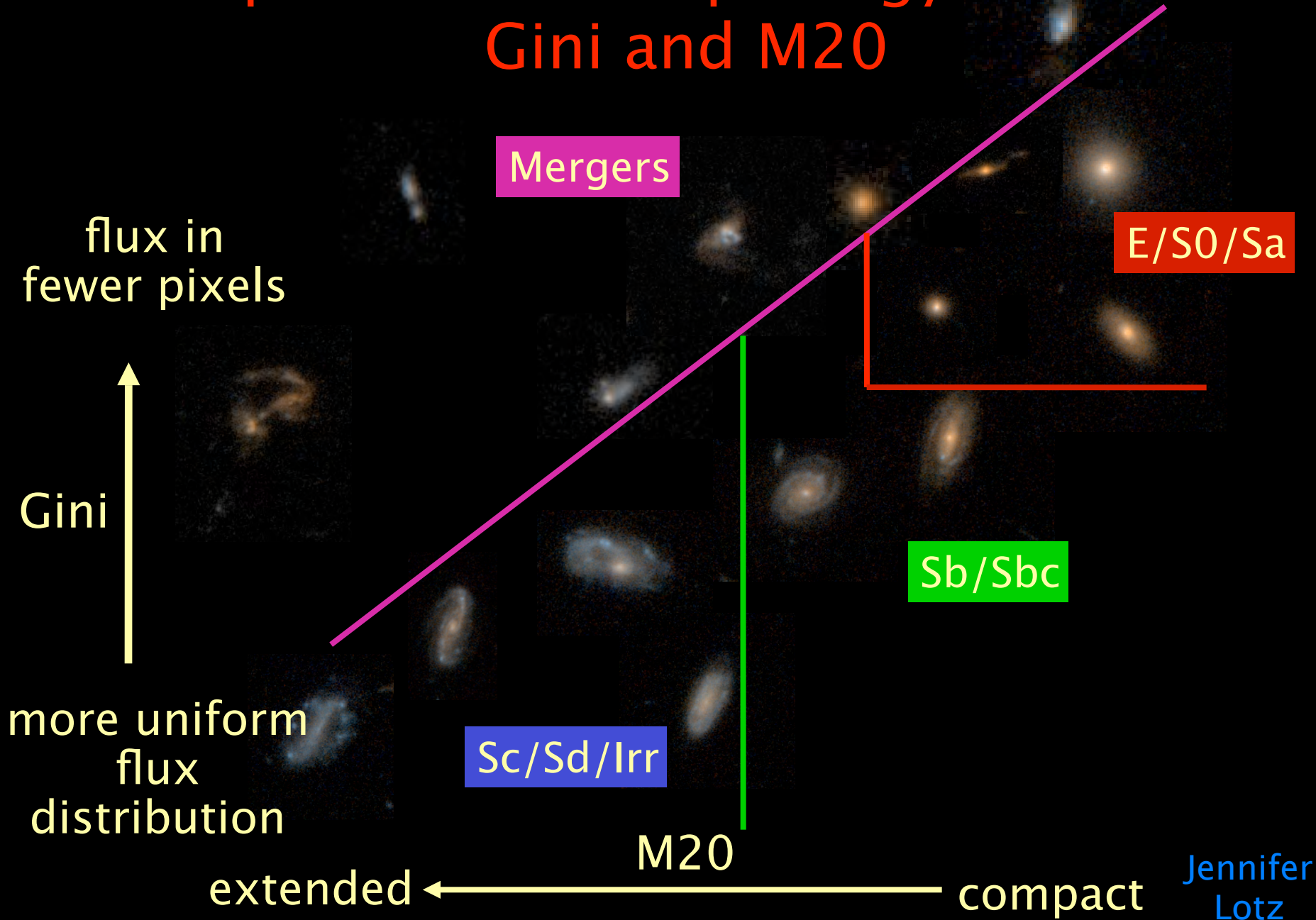
but does NOT assume particular geometry

- more sensitive to merger signatures (double nuclei)

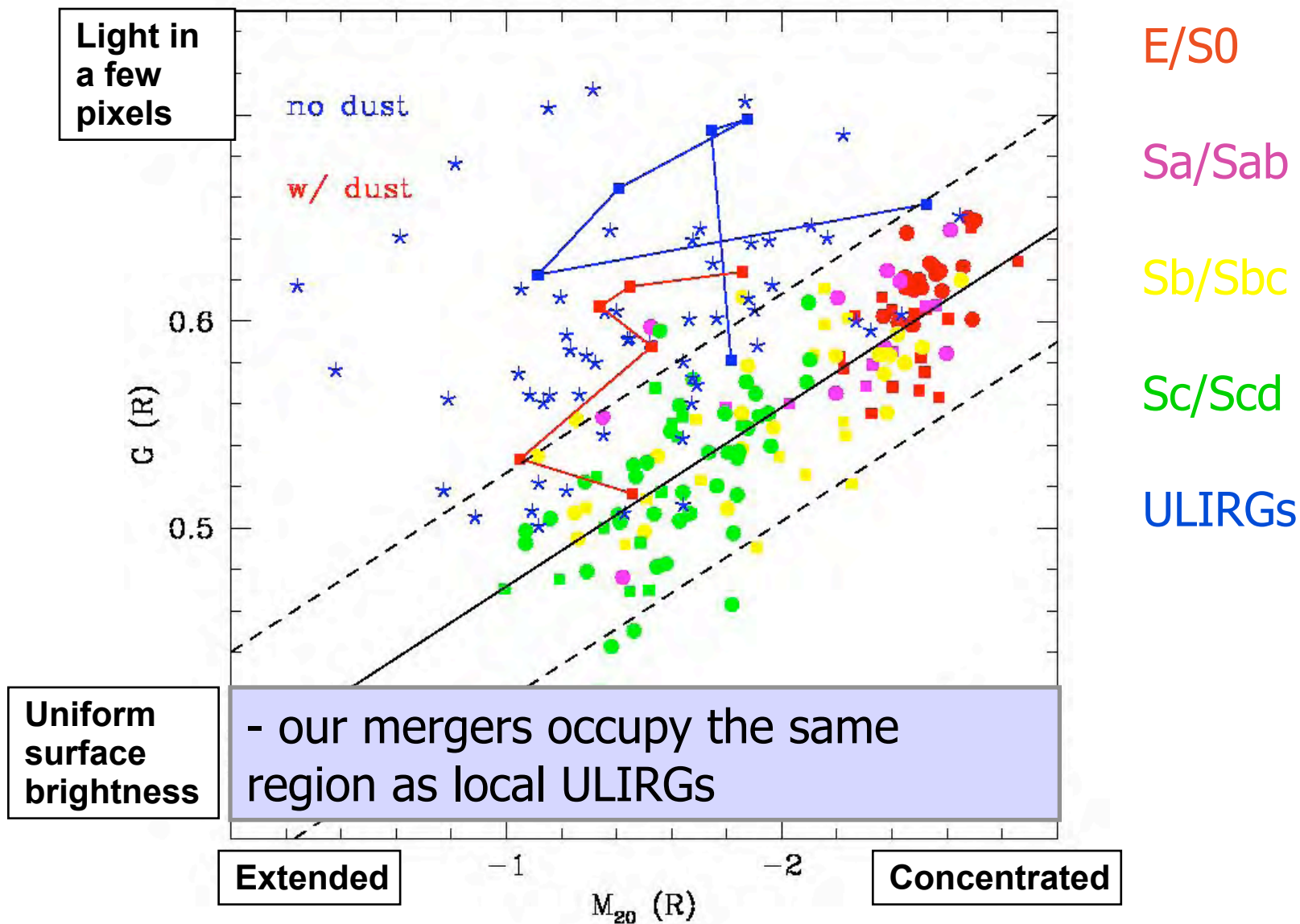
Local Galaxy G-M20 relation

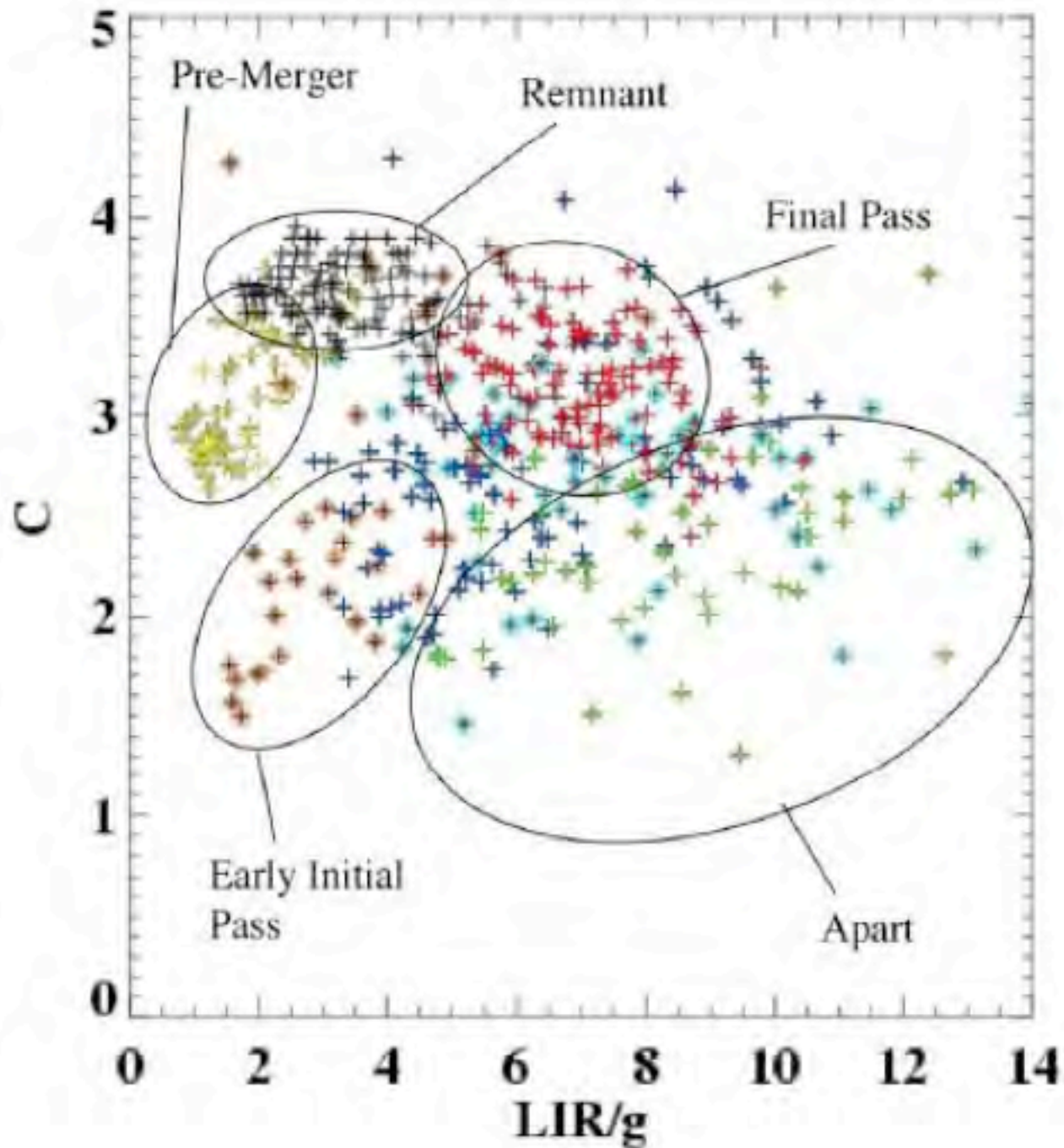


Nonparametric Morphology Measures Gini and M20



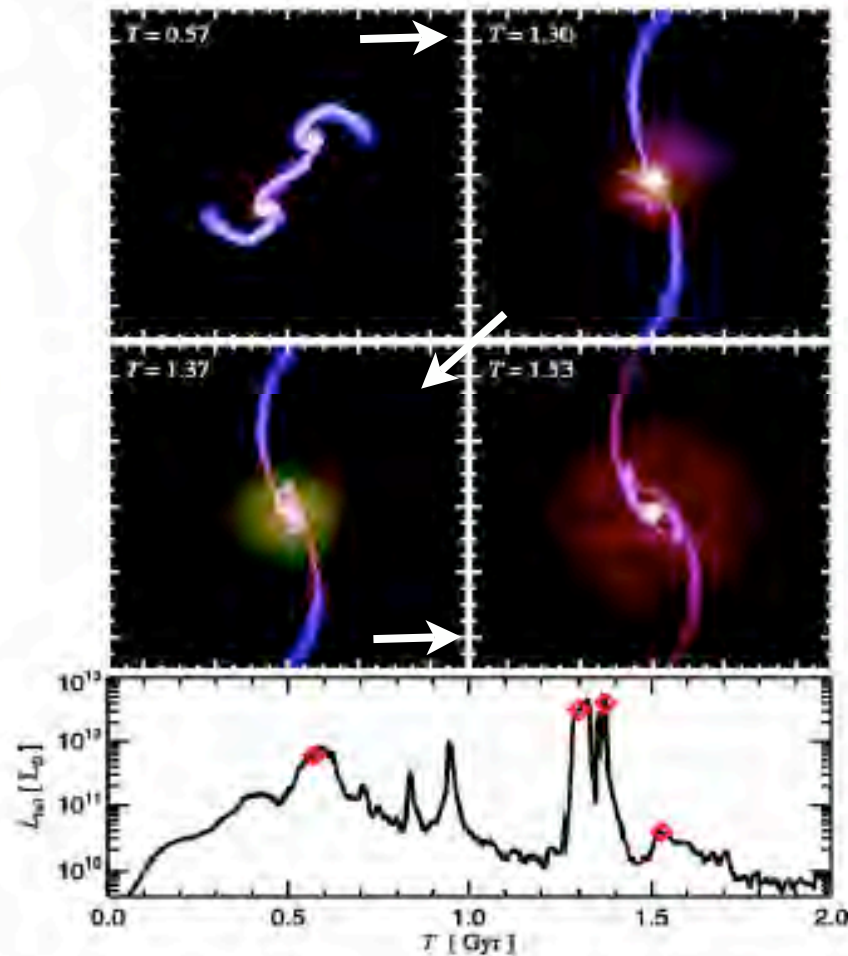
Modeling Merger Morphologies





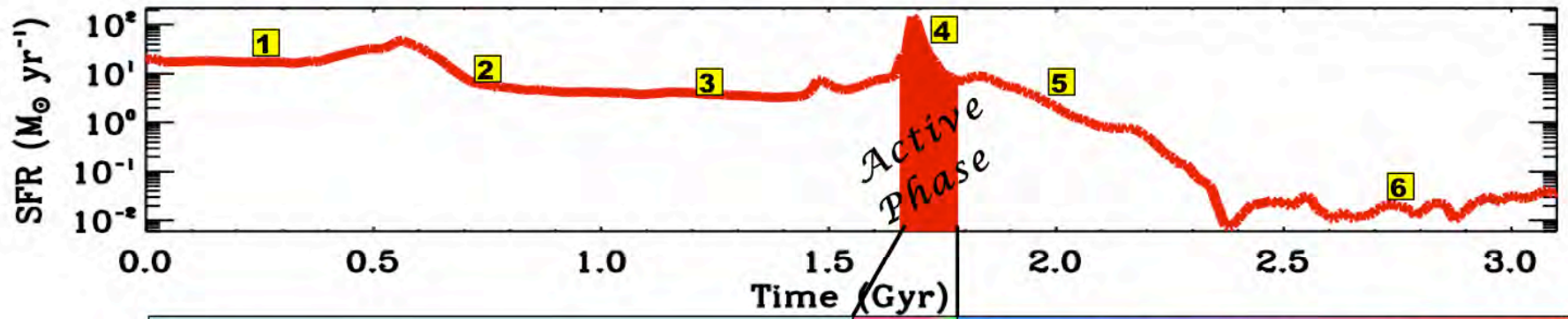
Using morphology and $\log L_{\text{IR}}/\text{optical}$ color, **it's possible to determine the merger stage of simulated galaxies** (senior thesis of Seth Cottrell, supervised by Lotz and Primack). We're now applying these techniques to a larger sample of simulations, and to observations. This will enable accurate measurement of merger rates. **Related 2008 senior thesis by Jared Rice.**

Merger Simulations with Supermassive Black Holes

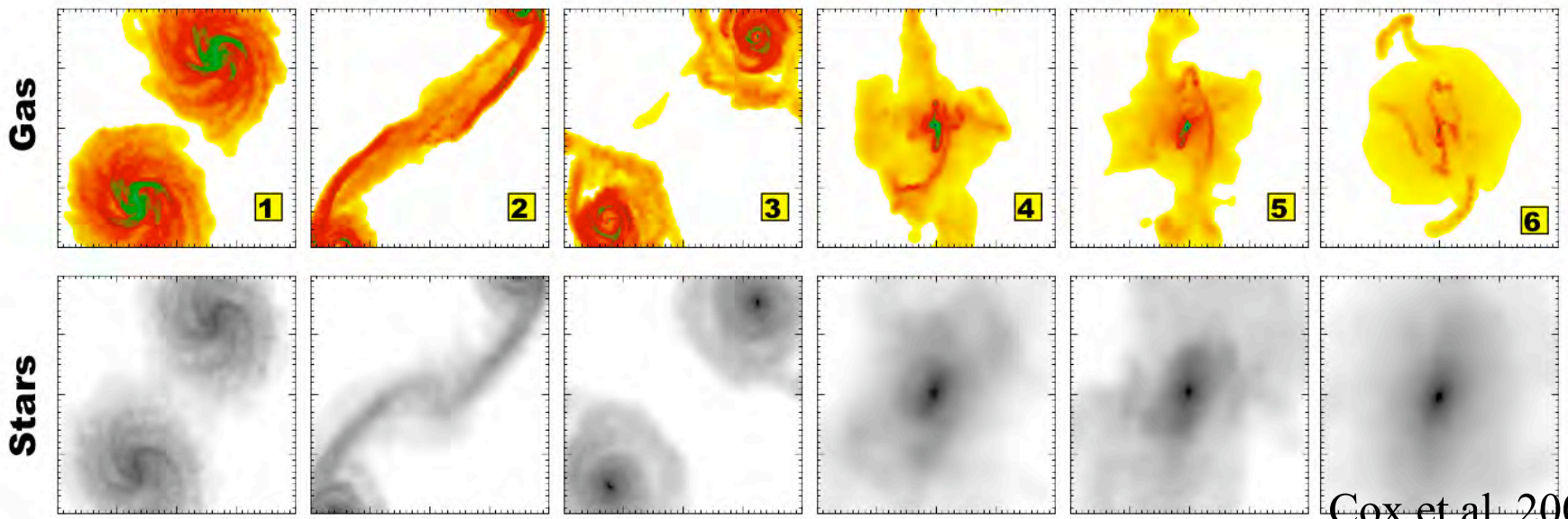


- ★ Mergers of gas-rich disk galaxies hosting SMBHs
- ★ Snapshots: gas densities at time (T) since interaction began
- ★ Plot: intrinsic bolometric luminosity (diamonds match snapshots)
- ★ Morphology most disturbed at $T \sim 1.30$ - 1.37 Gyrs.
- ★ AGNs turn on at $T \sim 1.30$ Gyr.

Proposed Co-Origin of Spheroids, SMBHs

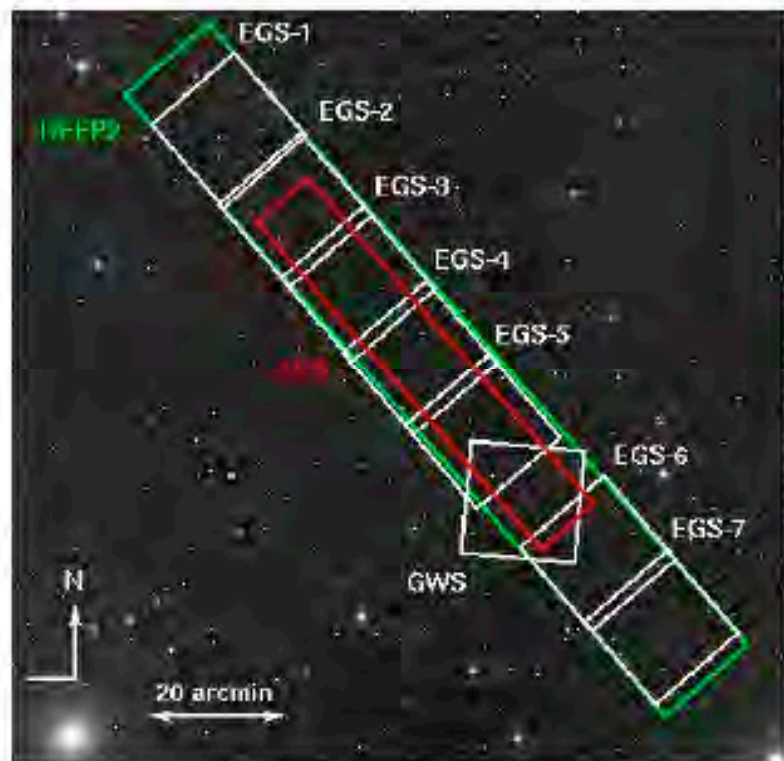


<p>Inspirational Stage</p> <ul style="list-style-type: none"> • multiple nuclei, tidal tails, bridges • the majority of stars are formed 	<p>Starburst-driven winds</p>	<p>(U)LIRG</p>	<p>QSO</p>	<p>Merger Remnant → Elliptical</p> <ul style="list-style-type: none"> • kinematics: tidal tails, shells, plumes & loops, kinematic subsystems • colors redden • formation of a hot gaseous halo • declining AGN activity • satisfies $M_{\text{BH}} - \sigma$ & FP
---	--------------------------------------	-----------------------	-------------------	---



Comparison with Observational Data

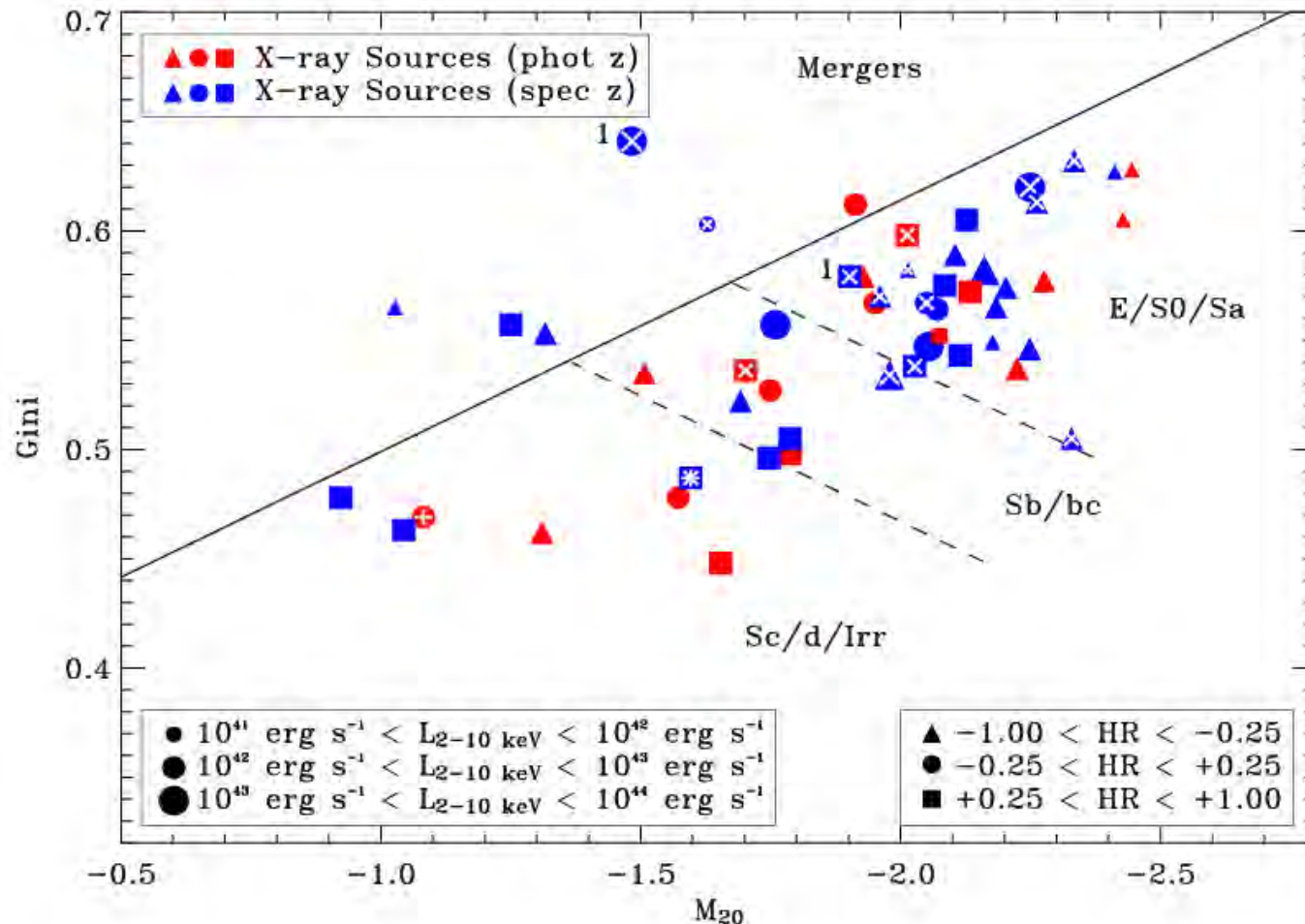
Extended Groth Strip (EGS)



- ✧ EGS: $\sim 0.5 \text{ deg}^2$ (green area)
- ✧ ACS: $\sim 0.33 \text{ deg}^2$ (red area)
- ✧ IRAC: $\sim 0.5 \text{ deg}^2$ (full EGS)
- ✧ Chandra: $\sim 3.75 \text{ sq. arcmin.}$ (Groth Westphal Strip; extra pointings now available)
- ✧ Canada-France-Hawaii Telescope Legacy Survey: photometric redshifts
- ✧ DEEP2 spectroscopic redshifts

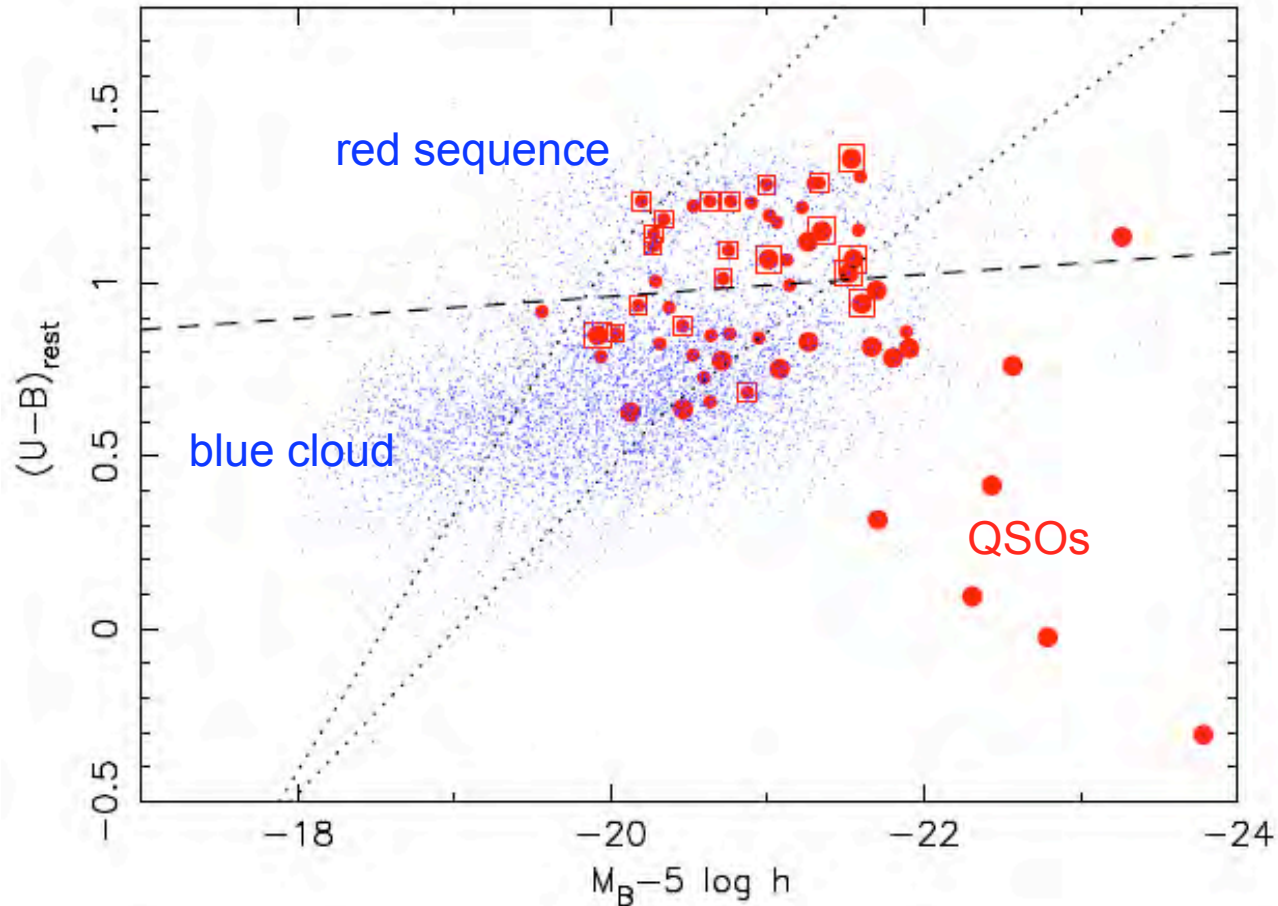
(<http://astro.ic.ac.uk/Research/Xray/egs/>)

Morphological distribution of EGS X-ray selected AGN



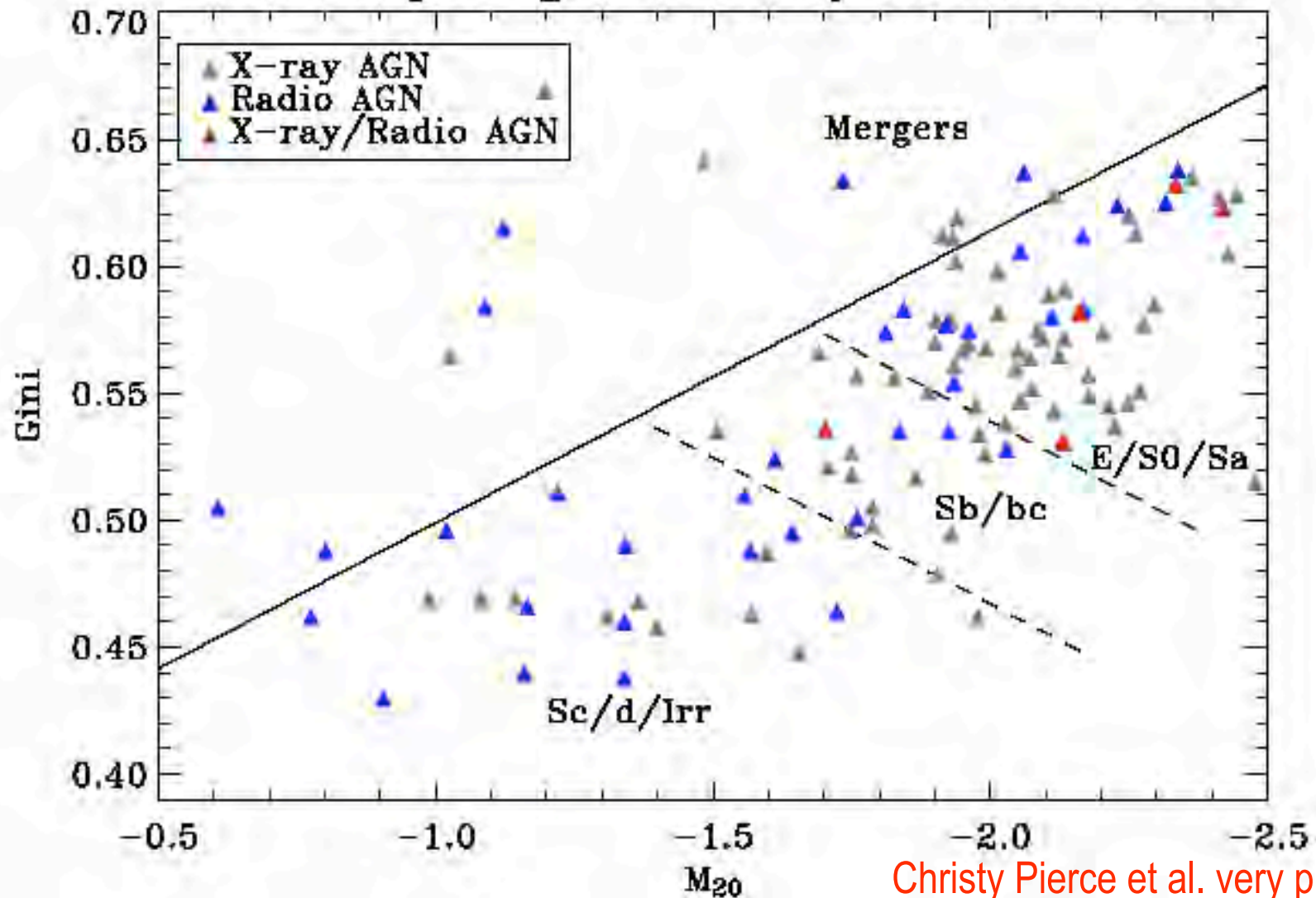
The highest fraction of EGS galaxies hosting AGN are early-types, not mergers. This suggests that the AGN activity is delayed, rather than occurring mainly during and immediately following mergers as the Hopkins et al. simulations predicted. (Christy Pierce et al., ApJ Letters, in press May 2007).

Color-Magnitude Diagram of EGS X-ray selected AGN



Rest-frame U-B colour is plotted against the B-band absolute magnitude for DEEP2 comparison galaxies (small blue dots) and X-ray sources (filled red circles) in the EGS in the range $0.7 < z < 1.4$. Squares around the symbols indicate hard X-ray sources, and more luminous systems ($L_x > 10^{43}$ erg s^{-1}) are plotted with larger symbols. The dashed line separates red and blue galaxies, and the dotted lines show the DEEP2 completeness limits at $z = 1.0$ and $z = 1.4$. (Kirpal Nandra et al., ApJ Letters, in press.)

EGS: Morphologies of X-ray and Radio AGN



Christy Pierce et al. very preliminary

Fig. 1.— X-ray and radio-selected AGN in the EGS. AGN outside of either the X-ray region or the radio region are excluded. Thus, each X-ray AGN represented should have been detectable by the radio survey, if there was any radio signal to detect, and vice versa. The host galaxies have $I \leq 23.5$, $0.2 \leq z < 1.2$, $r_P \geq 0.3$, $(S/N) \geq 2.5$, and are not flagged as non-contiguous (i.e., they meet the criteria for use with $G - M_{20}$). The colors represent method of selection, as shown.

Conclusions on EGS X-ray Selected AGN

We find that most X-ray selected AGN are hosted by early-type galaxies, based both on G-M20 and on visual classification. Mergers and Sb/bc galaxies are represented at the same rate as the field population, and Sc/d/Irr galaxies are greatly underrepresented. Close kinematic pairs are 3 times as likely to host X-ray AGN.

Most X-ray AGN are in the red sequence, in the top half of the blue cloud, or in the transition region between them. This supports the idea that AGN terminate star formation. But many transition galaxies do not have AGN.

Many X-ray AGN are bright ($>10^{42}$ erg/s) for 1 Gyr or more after a starburst. Many hard AGN are on the red sequence, disfavoring star-forming gas as a main source of obscuration.

Radio AGN appear to have similar morphology as X-ray AGN. Lack of enhanced likelihood of mergers suggests that bright AGN phase is delayed by ~100s of My after starburst peak.

THE END

Thanks for your patience!